An anion receptor that facilitates transmembrane proton-anion symport by deprotonating its sulfonamide N−H proton

Sopan Valiba Shinde, and Pinaki Talukdar*[a]

Department of Chemistry, Indian Institute of Science Education and Research Pune, Pune 411008, India. E-mail: ptalukdar@iiserpune.ac.in

Table of contents

SI. General Methods.

All chemicals, solvents and fluorescent dyes were purchased from commercial sources (Sigma-Aldrich, Alfa Aesar, Fisher Scientific, Spectrochem, and Avra). All commercial reagent grade chemicals were used as received without further purification unless otherwise specified. All deuterated solvents, HPTS dye, HEPES buffer, Triton X-100, sodium hydroxide and inorganic salts of molecular biology grade were obtained from Sigma-Aldrich. Egg-yolk phosphatidylcholine (EYPC) lipid as a solution in $CHCl_3$ (25 mg/mL), polycarbonate membrane (100 nm and 200 nm pore size), and mini-extruder used for vesicle preparation was obtained from Avanti Polar Lipids. All the Stock solutions were prepared in either HPLC grade DMSO, methanol or acetonitrile.

SII. Physical Measurements.

^{1}H-NMR spectra were recorded at 400 MHz using Bruker Ascend^{TM} 400 spectrometer, and ^{13}C NMR spectra using Jeol ECS-400 at 101 MHz frequency. All the spectra were calibrated with respect to residual solvent peaks. The following abbreviations were used to describe peak patterns wherever appropriate: br, broad; s, singlet; d, doublet; t, triplet; q, quartet; m, multiplet. All coupling constants (*J*) are reported in Hertz (Hz). High-resolution mass spectra (HRMS) were performed on an electron spray ionization time-of-flight (ESI-TOF). Melting points were measured with a micro melting point apparatus. Single Crystal X-Ray Diffraction (SCXRD) measurements were done on a Bruker KAPPA APEX II CCD diffractometer. Fluorescence spectra were recorded from Fluoromax-4 from JobinYvon Edison-equipped with an injector port and a magnetic stirrer. All buffer solutions were adjusted to required pH using a Helmer pH meter. All data from fluorescence studies were processed by either KaleidaGraph 3.51 or OriginPro 8.5 software.
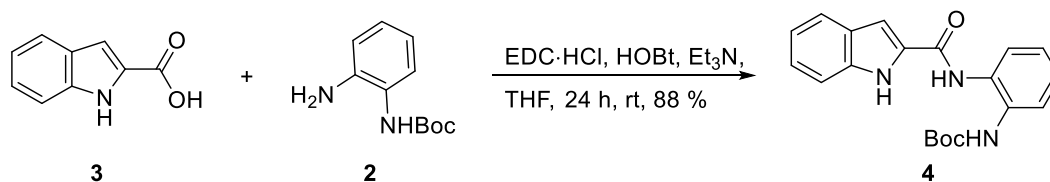
SIII. Synthesis.

Synthesis of *tert*-butyl (2-aminophenyl)carbamate 2:[S1]
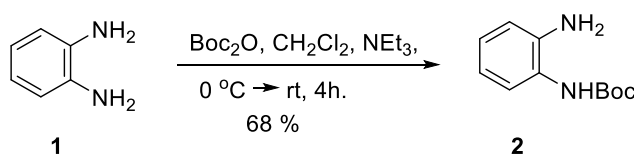
Scheme 1 Synthesis of *tert*-butyl (2-aminophenyl)carbamate **2**.

In a 100 mL round bottom flask, to a solution of *o*-phenylenediamine (1 g, 9.24 mmol) in CH$_2$Cl$_2$ (5 ml) was added di-*tert*-butyl bicarbonate (2.01 g, 9.24 mmol) and triethylamine (1.28 ml, 9.24 mmol) at 0 °C with continuous stirring. The reaction mixture stirred for 4 hours at 0 °C under N$_2$ atm. The reaction was quenched with water and the aqueous layer extracted with EtOAc (2 × 50 mL). The combined organic layers were dried over Na$_2$SO$_4$ and concentrated in *vacuo*. The solid residue was purified by column chromatography on SiO$_2$ (*Eluent*: Hexane: EtOAc from 91:9 to 88:12) to obtain **2** as a white solid (1.308 g, 67.94%).
^{1}H NMR (400 MHz, CDCl$_3$): δ = 7.27 (d, *J* = 7.8 Hz, 1H), 7.00 (td, *J* = 7.6, 1.5 Hz, 1H), 6.79 (td, *J* = 7.6, 1.4 Hz, 1H) 6.77 (dd, *J* = 7.8, 1.2 Hz, 1H), 3.70 (s, 1H), 1.51 (s, 9H); **HRMS** (ESI$^+$) *m/z*: [M + H]$^+$ calcd. for C$_{11}$H$_{17}$N$_2$O$_2$: 209.1290, found: 209.1292.

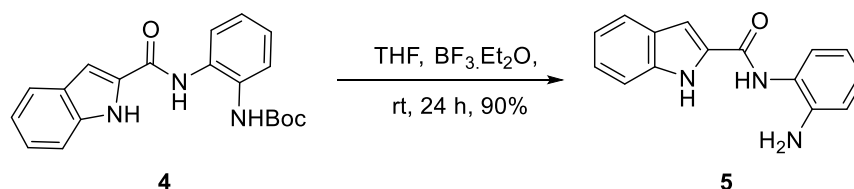**Synthesis of *tert*-butyl (2-(1*H*-indole-2-carboxamido) phenyl) carbamate (4):**

Scheme 2 Synthesis of *tert*-butyl (2-(1*H*-indole-2-carboxamido)phenyl)carbamate **4**.

In a 100 mL round-bottomed flask equipped with a magnetic stirrer, to a solution of Indole-2-carboxylic acid (835 mg, 5.185 mmol) in dry THF (10 mL) was added EDC·HCl (994 mg, 5.185 mmol) and 1- hydroxy benzotriazole (HOBt, 700 mg, 5.185 mmol) at room temperature and the reaction mixture stirred for 10 minutes. After 10 minutes, *tert*-butyl (2-aminophenyl) carbamate **1** (900 mg, 4.321 mmol) and triethylamine (656 mg, 6.481 mmol) were added at room temperature and the reaction mixture stirred for 24 hours. After completion of the reaction mixture was concentrated to remove excess THF, The water (50 mL) was added and the mixture was extracted with EtOAc (3 × 30 mL), the organic layers were separated, washed with brine, dried over anhydrous Na_2SO_4, filtered and concentrated under reduced pressure. The solid residue was purified by column chromatography on SiO_2 (*Eluent*: Hexane:EtOAc 91:9) to obtain **4** as a white solid (1.33 g, 87.8 %).

M.p.: 194 °C; **^{1}H NMR** (400 MHz, $CDCl_3$): δ = 9.36 (s, 1H), 7.83 (d, *J* = 8.0 Hz, 1H), 7.66 (d, *J* = 8 Hz, 1H) 7.44 (d, *J* = 8.3 Hz, 1H), 7.34 – 7.13 (m, 7H), 7.09 (s, 1H), 6.75 (s, 1H), 1.56 (s, 9H); **^{13}C NMR** (101 MHz, $CDCl_3$): δ = 160.3, 154.8, 136.8, 130.9, 130.4, 130.0, 127.9, 126.2, 126.1, 125.9, 124.9, 124.5, 122.2, 120.8, 112.2, 103.6, 81.8, 28.5 (3C); **HRMS** (ESI$^+$) *m/z*: [M + Na]$^+$ calcd. for $C_{20}H_{21}N_3NaO_3$: 374.1481, found: 374.1481.

Synthesis of *N*-(2-aminophenyl)-1*H*-indole-2-carboxamide (3):
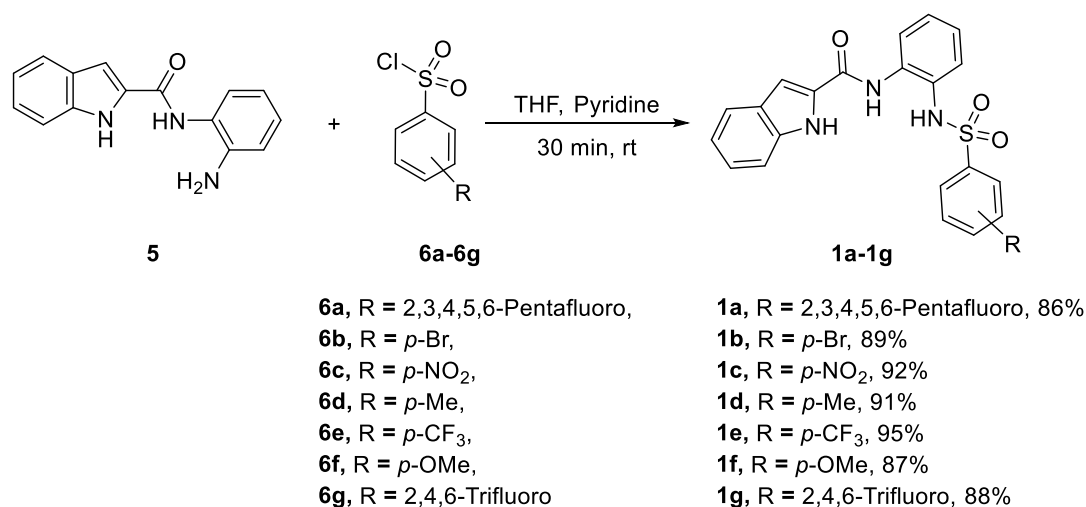

Scheme 3 Synthesis of *N*-(2-aminophenyl)-1*H*-indole-2-carboxamide **5**.

In a 100 mL round bottom flask, to a solution of *tert*-butyl (2-(1*H*-indole-2-carboxamido) phenyl) carbamate **4** (740 mg) in THF (5 mL) was added BF$_3$·OEt$_2$ (98%, 6 mL) was added at room temperature. The reaction mixture was stirred for 24 hours (followed by TLC). After

completion of the reaction the THF was removed in *vacuo*. To the liquid residue, water (5 ml) was added. The excess of BF$_3$·OEt$_2$ was quenched with the dropwise addition of saturated NaHCO$_3$ until the effervescence of CO$_2$ stops. The mixture extracted with ethyl acetate (50 mL × 2), the organic layer separated, dried over Na$_2$SO$_4$, filtered and concentrated in *vacuo*. The residue was purified by column chromatography on SiO$_2$ (*Eluent*: 1% MeOH in CH$_2$Cl$_2$) to obtain **5** as a yellowish solid (510 mg, 96.5 %).

M.p.: 206 °C; **¹H NMR** (400 MHz, DMSO-*d₆*): δ = 11.69 (s, 1H), 9.68 (s, 1H), 7.65 (d, *J* = 8.0 Hz, 1H), 7.46 (d, *J* = 8.3 Hz, 1H), 7.36 (s, 1H), 7.21 (td, *J* = 6.2, 1.1 Hz, 2H), 7.06 (t, *J* = 7.5 Hz, 1H), 6.99 (t, 7.6 Hz, 1H), 6.81 (dd, *J* = 8.0, 1.2 Hz, 1H), 6.63 (td, *J* = 7.7, 1.3 Hz, 1H), 4.95 (s, 2H); **¹³C NMR** (101 MHz, DMSO-*d₆*): δ = 159.8, 143.2, 136.6, 131.5, 127.1, 126.7, 126.5, 123.5, 122.9, 121.6, 119.8, 116.3, 116.2, 112.3, 103.6; **HRMS** (ESI⁺) *m/z*: [M + H]⁺ calcd. for C$_{15}$H$_{14}$N$_3$O: 252.1137, found: 252.1144.

General Procedure for Synthesis of Transporter 1a - 1g:

6a, R = 2,3,4,5,6-Pentafluoro,
6b, R = *p*-Br,
6c, R = *p*-NO$_2$,
6d, R = *p*-Me,
6e, R = *p*-CF$_3$,
6f, R = *p*-OMe,
6g, R = 2,4,6-Trifluoro

1a, R = 2,3,4,5,6-Pentafluoro, 86%
1b, R = *p*-Br, 89%
1c, R = *p*-NO$_2$, 92%
1d, R = *p*-Me, 91%
1e, R = *p*-CF$_3$, 95%
1f, R = *p*-OMe, 87%
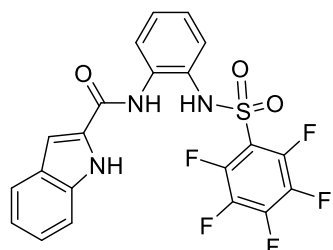**1g,** R = 2,4,6-Trifluoro, 88%

Scheme 4 General synthesis of transporter **1a – 1g**.

In 10 mL round bottom flask, to a stirred suspension of *N*-(2-aminophenyl)-1*H*-indole-2-carboxamide **5** (50 mg, 0.199 mmol) and Aryl sulfonyl chloride **6a - 6g** (0.298 mmol) in dry THF (1 mL) was added pyridine (1 mL). The reaction mixture was stirred for 30 minutes at room temperature. THF was removed under vacuum, and the residue was taken in 4M HCl, extracted with ethyl acetate (10 mL × 2). The organic layer separated, dried over Na$_2$SO$_4$,

filtered and concentrated in *vacuo*. The residue was purified by column chromatography (*Eluent*: 1% MeOH in CH$_2$Cl$_2$) to obtain product **1a–1g** in 86 – 92% yield.
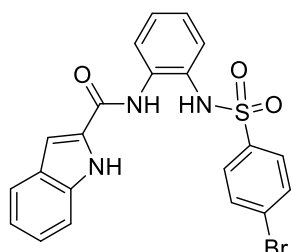
N-(2-((perfluorophenyl)sulfonamido)phenyl)-1H-indole-2-carboxamide (1a): Beige color solid; **M.p.:** 286 °C; **^{1}H NMR** (400 MHz, DMSO-d_6): δ = 11.75 (s, 1H), 10.35 (s, 1H), 9.66 (s, 1H), 7.70 (d, *J* = 8.0 Hz, 1H), 7.56 (d, *J* = 7.88 Hz, 1H), 7.48(d, J = 6.24 Hz, 1H), 7.44 – 7.37 (m, 1H), 7.31 (td, *J* = 7.34, 1.46 Hz, 1H), 7.25 (td, *J* = 7.58, 1.06 Hz, 1H), 7.20 (d, *J* = 1.5 Hz, 1H), 7.09 (t, *J* = 7.46 Hz, 1H); **^{13}C NMR** (101 MHz, DMSO-d_6): δ = 159.7, 143.7 (dm, *J* = 242 Hz), 137.3 (dm, 252 Hz), 137.1, 132.8, 130.0, 129.0, 128.3, 127.6, 126.9, 126.3, 126.2, 124.2, 121.8, 121.1, 115.3 (t, 14 Hz), 112.5, 103.8; **HRMS** (ESI$^+$) *m/z*: [M + H]$^+$ calcd. for C$_{21}$H$_{13}$F$_5$N$_3$O$_3$S: 482.0598, found: 482.0595.

N-(2-((4-bromophenyl)sulfonamido)phenyl)-1H-indole-2-carboxamide (1b): White solid; **M.p.:** 264 °C; **^{1}H NMR** (400 MHz, DMSO-d_6): δ = 11.78 (s, 1H), 9.80 (s, 1H), 9.58 (s, 1H), 7.75 (dd, *J* = 8.12, 1.12 Hz, 1H), 7.72 (d, *J* = 8.08 Hz, 1H), 7.60 – 7.44 (m, 5H), 7.34 – 7.21 (m, 2H), 7.20 – 7.07 (m, 4H); **^{13}C NMR** (101 MHz, DMSO-d_6): δ = 159.6, 138.5, 137.0, 132.8, 132.3, 130.7, 128.5, 128.0, 127.5, 127.1, 126.9 (2C), 125.5, 124.7, 124.1, 121.9, 120.1, 112.5, 103.9; **HRMS** (ESI$^+$) *m/z*: [M + H]$^+$ calcd. for C$_{21}$H$_{17}$BrN$_3$O$_3$S: 470.0174, found: 470.0176.
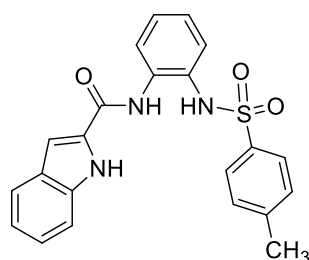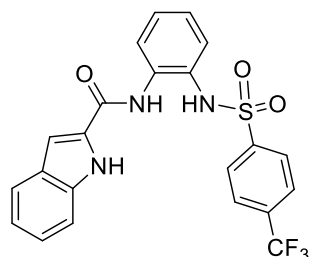
N-(2-((4-nitrophenyl)sulfonamido)phenyl)-1H-indole-2-carboxamide (1c): Light brown color solid; **M.p.:** 295 °C; **^{1}H NMR** (400 MHz, DMSO-d_6): δ = 11.68 (s, 1H), 9.95 (s, 1H), 9.45 (s, 1H), 8.05 (d, *J* = 8.7 Hz, 2H), 7.79 (d, *J* = 8.7 Hz, 2H), 7.67 (dd, *J* = 16.5, 8.0 Hz, 2H), 7.45 (d, *J* = 8.3 Hz, 1H), 7.39 – 7.30 (m, 1H), 7.28 – 7.18 (m, 3H), 7.14 – 7.06 (m, 2H); **^{13}C NMR** (101 MHz, DMSO-d_6): δ = 159.5, 149.4,
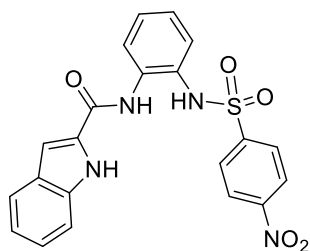
144.8, 136.9, 132.8, 130.5, 128.0 (2C), 127.9, 127.6, 126.8, 125.8, 125.4, 124.5, 124.5, 121.8, 120.1, 112.5, 104.0; **HRMS** (ESI$^+$) *m/z*: [M + H]$^+$ calcd. for $C_{21}H_{17}N_4O_5S$: 437.0919, found: 437.0915.
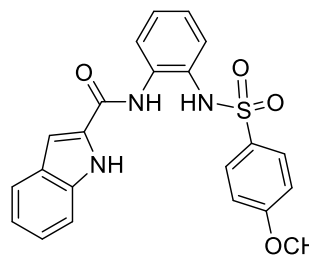
N-(2-((4-methylphenyl)sulfonamido)phenyl)-1H-indole-2-carboxamide **(1d):**. White solid; **M.p.:** 230 °C; **^{1}H NMR** (400 MHz, DMSO-d_6): δ = 11.79 (s, 1H), 9.69 (s, 1H), 9.55 (s, 1H), 7.72 (d, *J* = 7.96 Hz, 1H), 7.72 (d, *J* = 8.04 Hz, 2H), 7.49 (m, 3H), 7.32 – 7.22 (m, 2H), 7.19 – 7.06 (m, 6H), 2.21 (s, 3H); **^{13}C NMR** (101 MHz, DMSO-d_6): δ = 160.0, 143.8, 137.4, 137.0, 133.2, 131.4, 130.1, 128.6, 127.5, 127. 4 (2C), 127.1, 125.7, 124.9, 124.5, 122.3, 120.6, 113.0, 104.2, 21.4; **HRMS** (ESI$^+$) *m/z*: [M + H]$^+$ calcd. for $C_{22}H_{21}N_3O_3S$: 406.1225, found: 406.1226.

N-(2-((4-(trifluoromethyl)phenyl)sulfonamido)phenyl)-1H-indole-2-carboxamide **(1e):** White solid; **M.p.:** 234 °C; **^{1}H NMR** (400 MHz, DMSO-d_6): δ = 11.72 (s, 1H), 9.91 (s, 1H), 9.53 (s, 1H), 7.80 (d, *J* = 8.2 Hz, 2H), 7.76 – 7.66 (m, 4H), 7.47 (d, *J* = 8.3 Hz, 1H), 7.34 – 7.28 (m, 1H), 7.24 (t, *J* = 7.5 Hz, 1H), 7.21 – 7.15 (m, 2H), 7.14 – 7.06 (m, 2H); **^{13}C NMR** (101 MHz, DMSO-d_6): δ = 159.6, 143.3, 137.0, 132.8, 132.2 (q, *J* = 33 Hz, *C*CF$_3$), 130.6, 127.9, 124.4, 127.4, 126.9, 126.5, 126.4, 125.6, 124.9, 124.1, 123.2 (q, *J* = 272 Hz, *CF$_3$*), 121.8, 120.1, 112.5, 103.9; **HRMS** (ESI$^+$) *m/z*: [M + H]$^+$ calcd. for $C_{22}H_{17}F_3N_3O_3S$: 460.0942, found: 460.0948.

N-(2-((4-methoxyphenyl)sulfonamido)phenyl)-1H-indole-2-carboxamide **(1f):** Pale yellow solid; **M.p.:** 231 °C; **^{1}H NMR** (400 MHz, DMSO-d_6) δ = 11.81 (s, 1H), 9.62 (s, 1H), 9.59 (s, 1H), 7.78 (d, *J* = 7.24 Hz, 1H), 7.72 (d, *J* = 7.96 Hz, 1H), 7.54 (d, *J* = 8.9 Hz, 2H), 7.49 (d, *J* = 8.3 Hz, 1H), 7.31 – 7.23 (m, 2H), 7.18 (d, *J* = 1.5 Hz, 1H), 7.16 – 7.05 (m, 3H), 6.86 (d, *J* = 8.9 Hz, 2H), 3.66 (s, 3H); **^{13}C NMR** (101

MHz, DMSO-d_6) δ 162.4, 159.5, 136.9, 132.8, 130.9, 130.8, 128.8, 128.2, 127, 126.9 (2C), 125.2, 124.2, 124.0, 121.9, 120.1, 114.3, 112.5, 103.7, 55.5; **HRMS** (ESI$^+$) *m/z*: [M + H]$^+$ calcd. for C$_{22}$H$_{20}$N$_3$O$_4$S: 422.1174, found: 422.1178.

N-(2-((2,4,6-trifluorophenyl)sulfonamido)phenyl)-1H-indole-2-carboxamide (1g): yellow
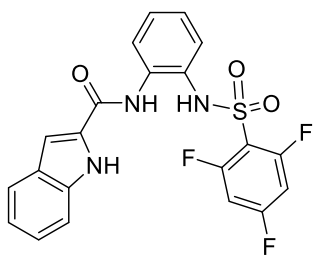
Orange colored solid; **M.p.:** 238 – 239 °C; **¹H NMR** (400 MHz, DMSO-d_6): δ = 11.81 (s, 1H), 10.06 (s, 1H), 9.79 (s, 1H), 7.72 (d, *J* = 8.0 Hz, 1H), 7.64 (d, *J* = 8.1 Hz, 1H), 7.49 (d, *J* = 8.3 Hz, 1H), 7.35 – 7.30 (m, 2H), 7.28 – 7.21 (m, 3H), 7.15 – 7.05 (m, 3H); **¹³C NMR** (101 MHz, DMSO-d_6) δ 164.7 (dt, *J* = 256.4, 16.2 Hz), 156.2

(dm, *J* = 259.3 Hz, 2C) 137.0, 132.6, 130.5, 127.6, 127.4, 127.0, 125.9, 125.2, 124.2, 121.9, 120.1, 114.0 (dt, *J* = 16.9, 4.8 Hz), 112.6, 104.0, 102.5 (t, *J* = 27.2 Hz); HRMS (ESI$^+$) *m/z*: [M + H]$^+$ calcd. for C$_{21}$H$_{15}$F$_3$N$_3$O$_3$S: 446.0786, found: 446.0785.

SIV. Supporting NMR Spectra
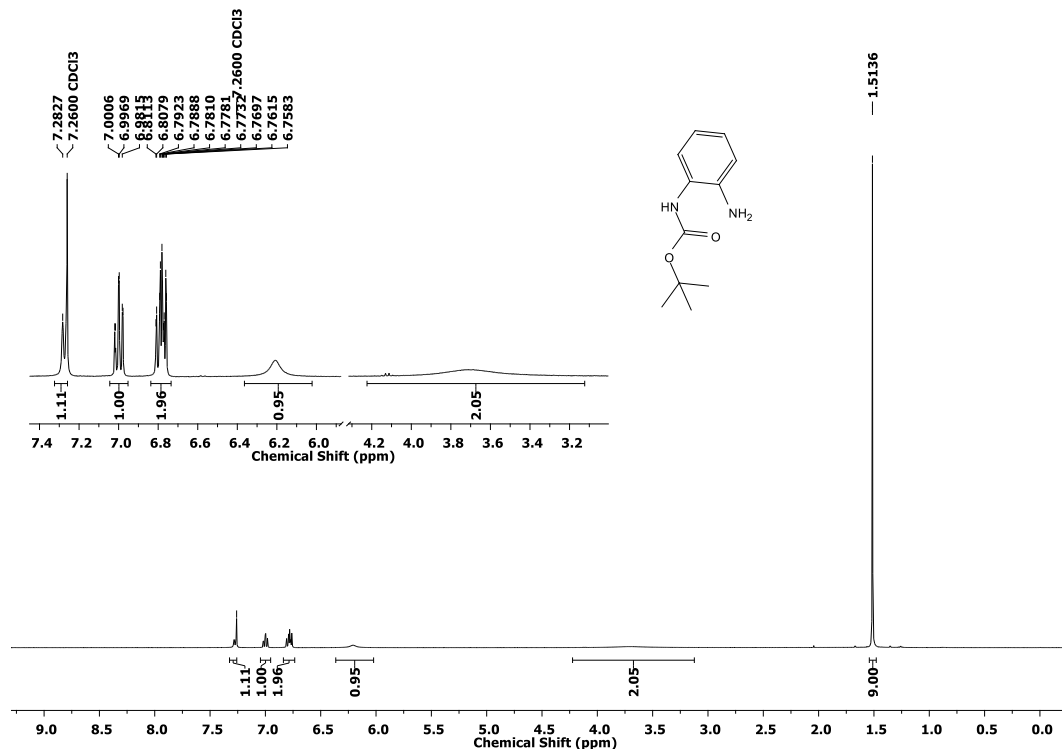
Fig. S1 ¹H NMR spectrum of *tert*-butyl (2-aminophenyl)carbamate **2**.
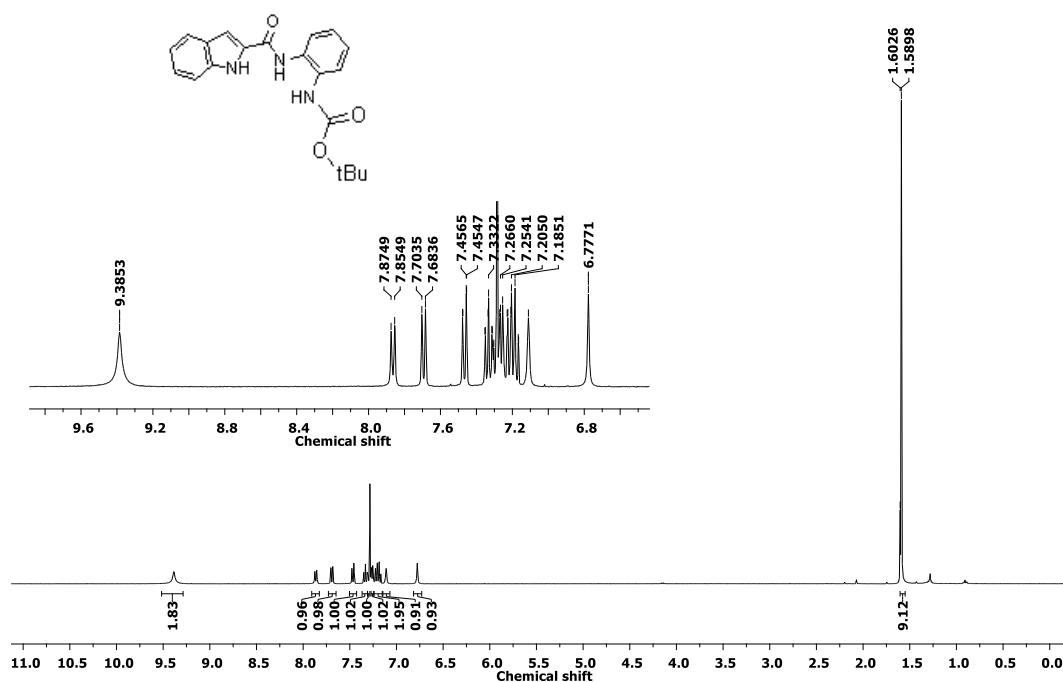
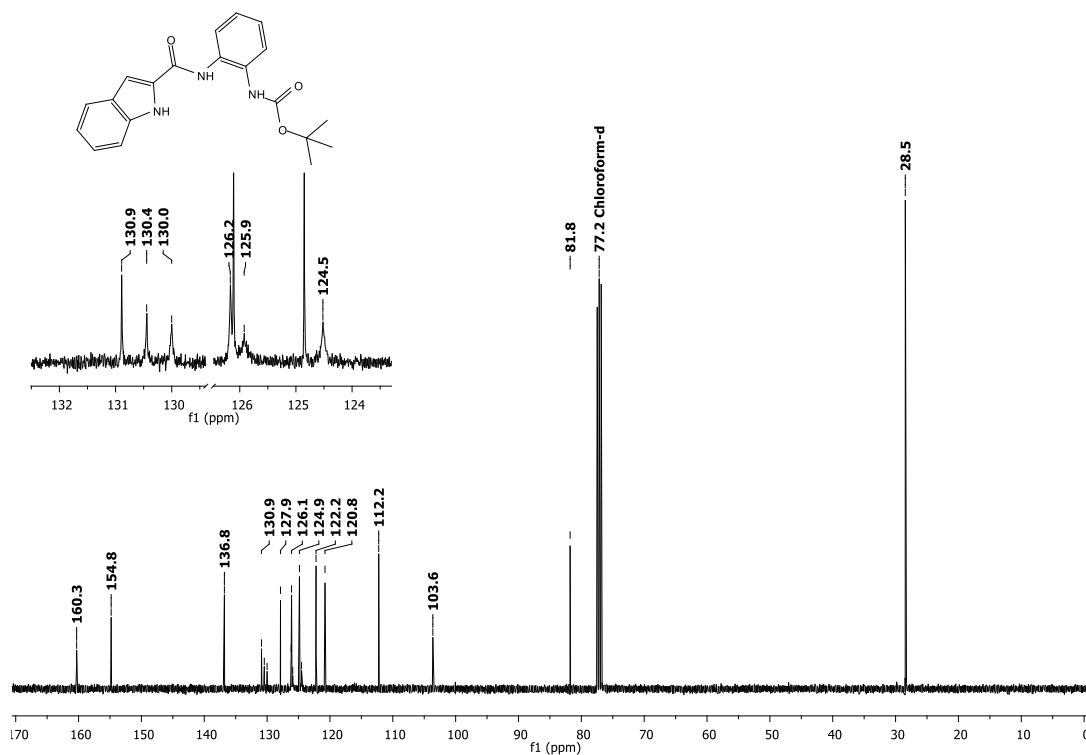**Fig. S2** ^{1}H NMR spectrum of *tert*-butyl (2-(1*H*-indole-2-carboxamido)phenyl)carbamate **4**.

Fig. S3 ^{13}C NMR spectrum of *tert*-butyl (2-(1*H*-indole-2-carboxamido)phenyl)carbamate **4**.
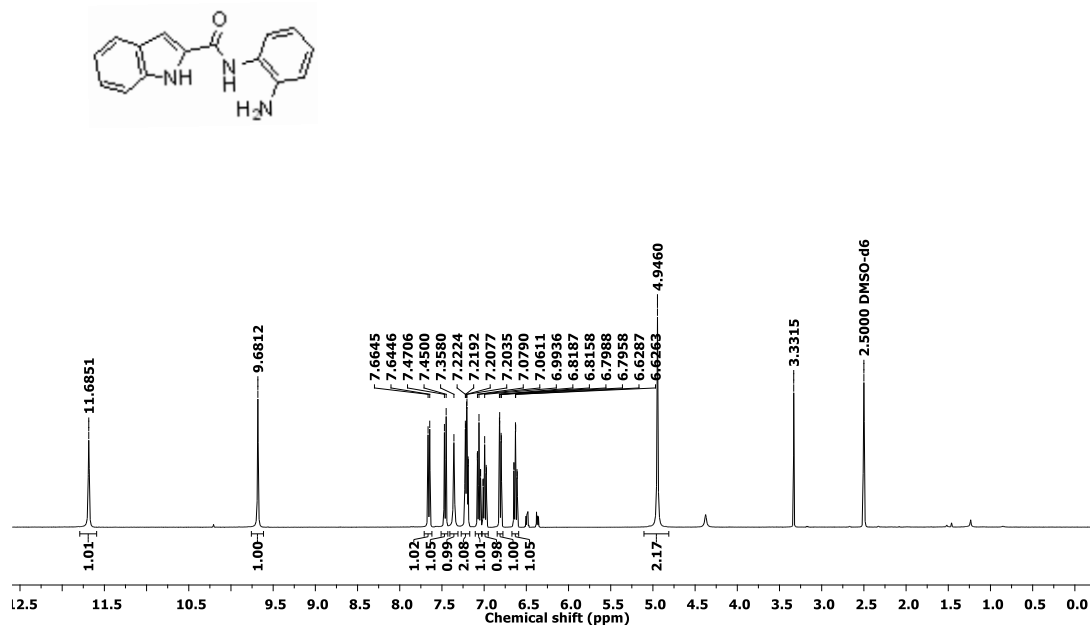
Fig. S4 ^{1}H-NMR spectrum of *N*-(2-aminophenyl)-1*H*-indole-2-carboxamide **5**.
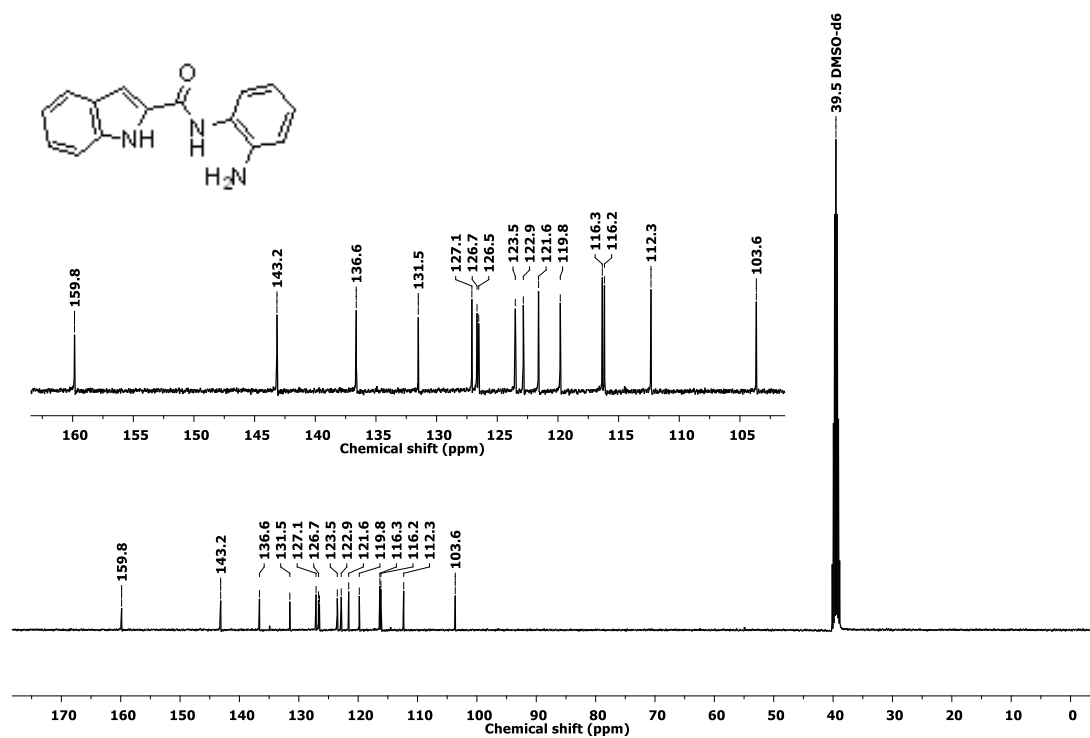

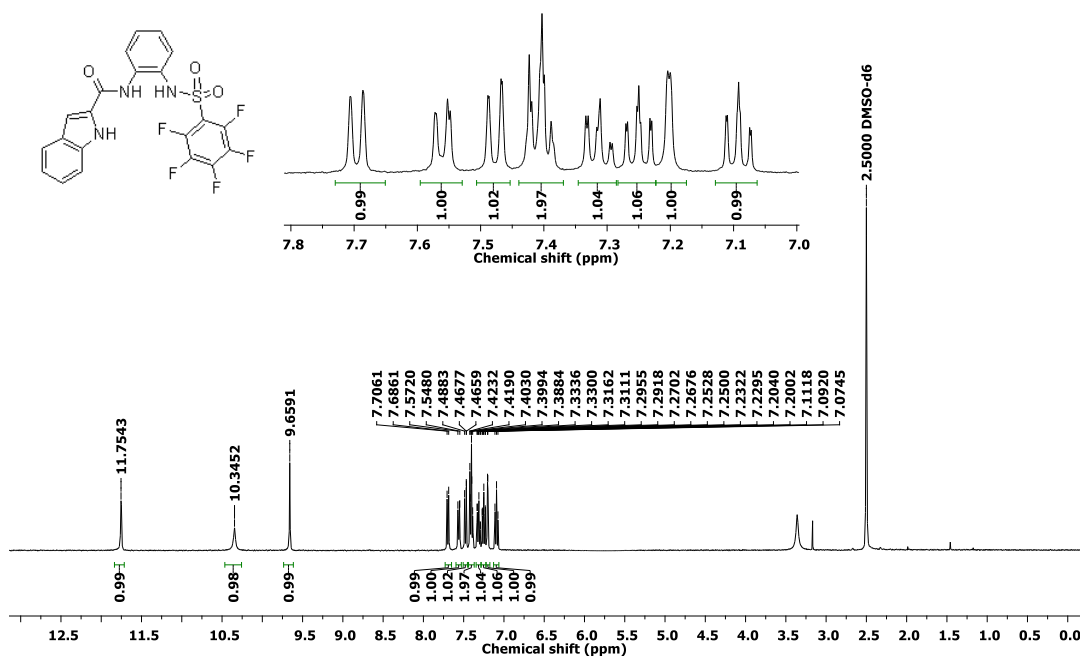**Fig. S5** ^{13}C NMR spectrum of *N*-(2-aminophenyl)-1*H*-indole-2-carboxamide **5**.

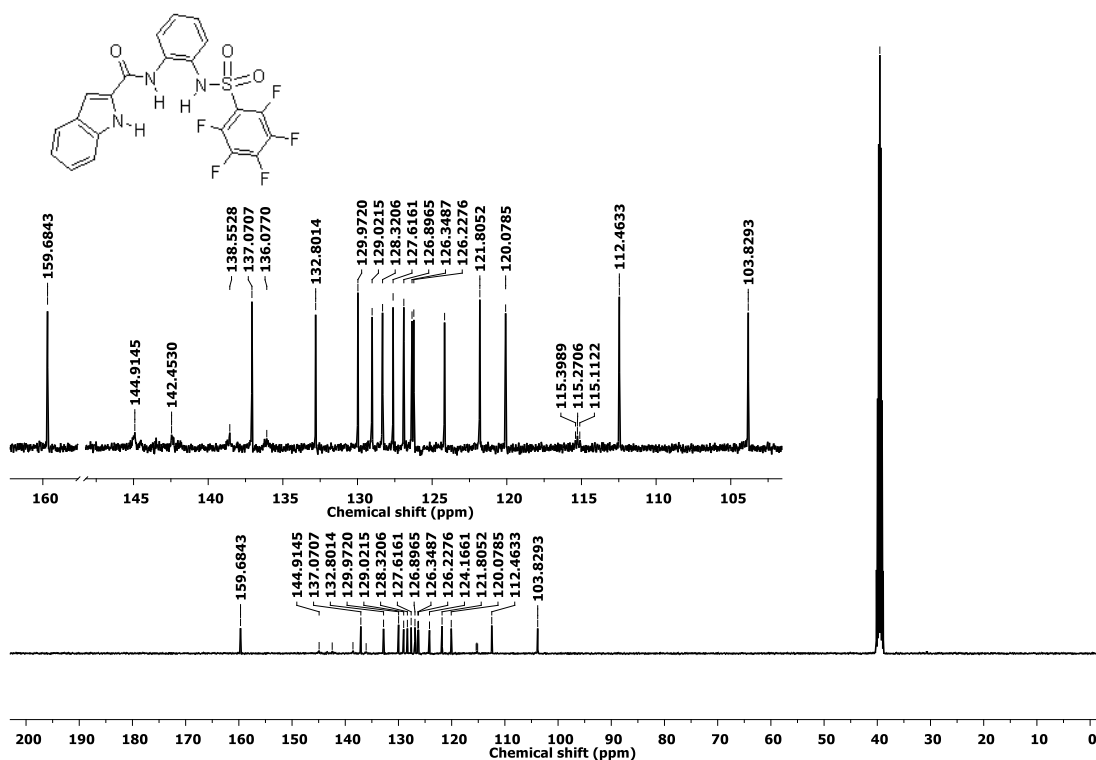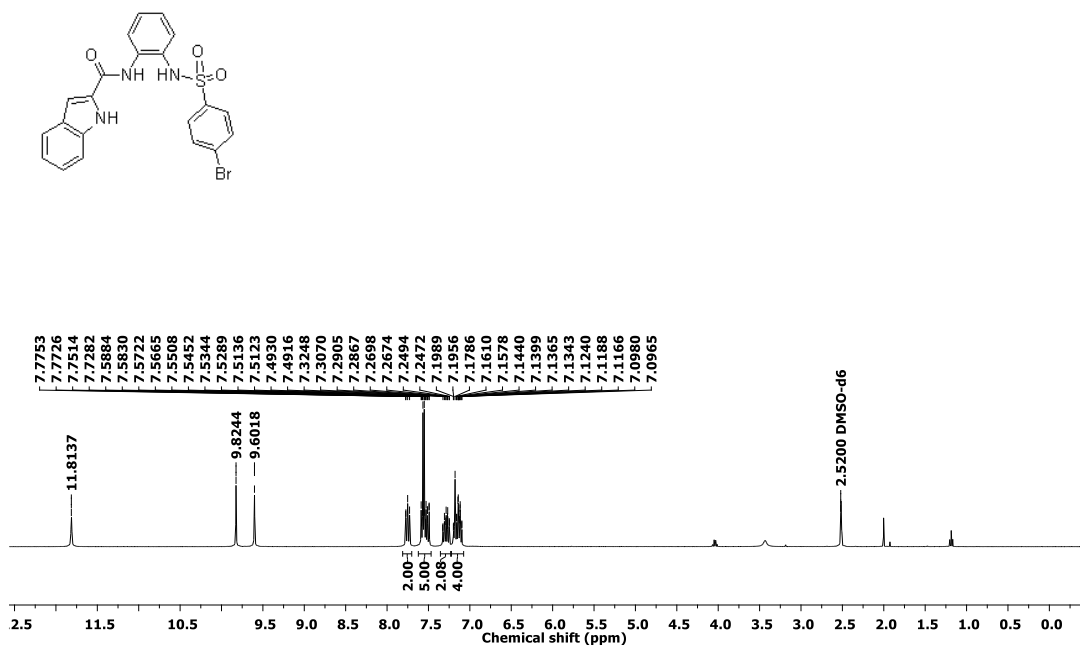**Fig. S6** ^{1}H NMR spectrum of *N*-(2-((perfluorophenyl)sulfonamido)phenyl)-1*H*-indole-2-carboxamide **1a**.

Fig. S7 ^{13}C NMR spectrum of *N*-(2-((perfluorophenyl)sulfonamido)phenyl)-1*H*-indole-2-carboxamide **1a.**

Fig. S8 ^{1}H NMR spectrum of *N*-(2-((4-bromophenyl)sulfonamido)phenyl)-1*H*-indole-2-carboxamide **1b**.
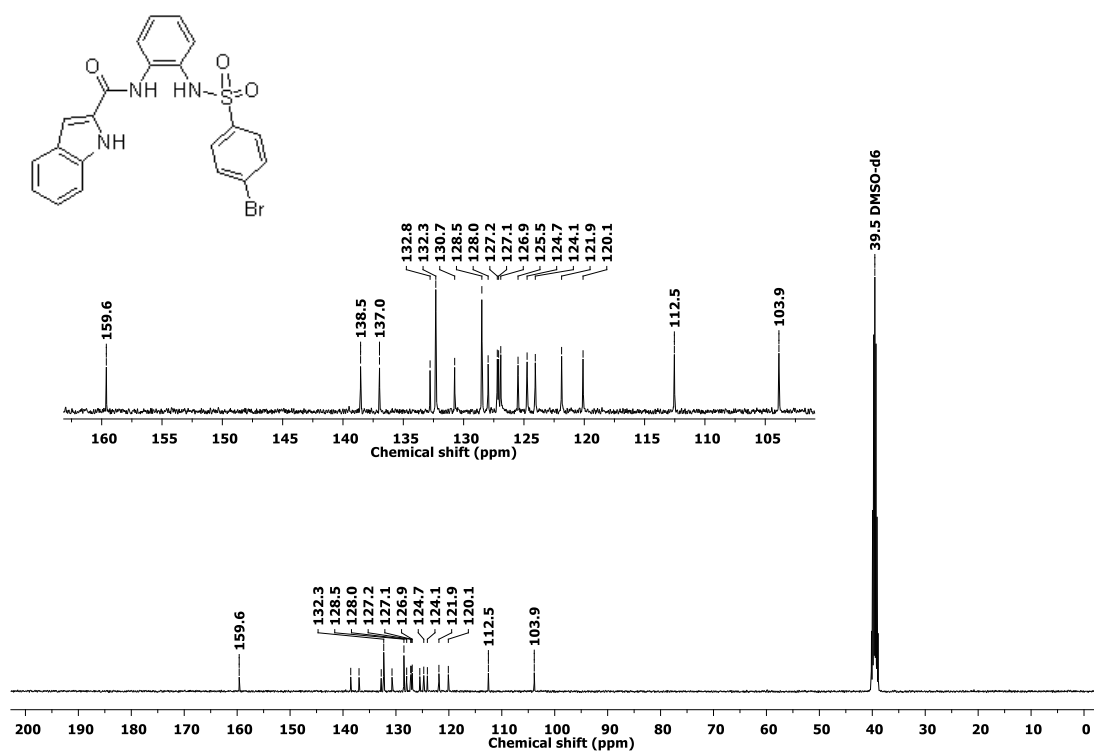

Fig. S9 ^{13}C NMR spectrum of *N*-(2-((4-bromophenyl)sulfonamido)phenyl)-1*H*-indole-2-carboxamide **1b**.
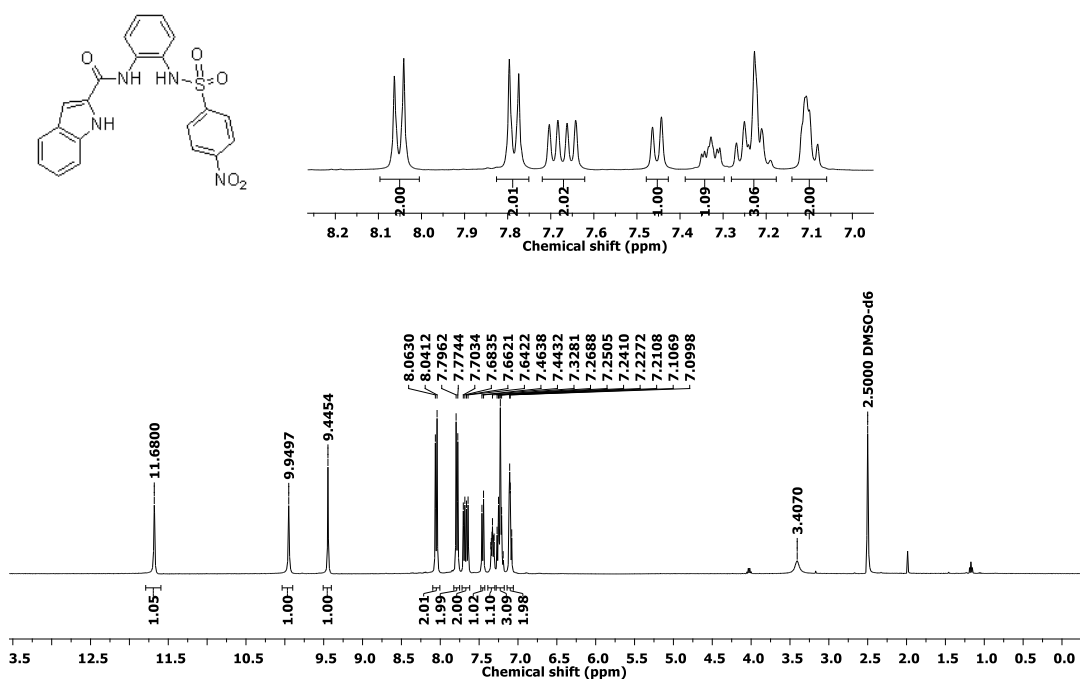
Fig. S10 ^{1}H NMR spectrum of *N*-(2-((4-nitrophenyl)sulfonamido)phenyl)-1*H*-indole-2-carboxamide **1c**.
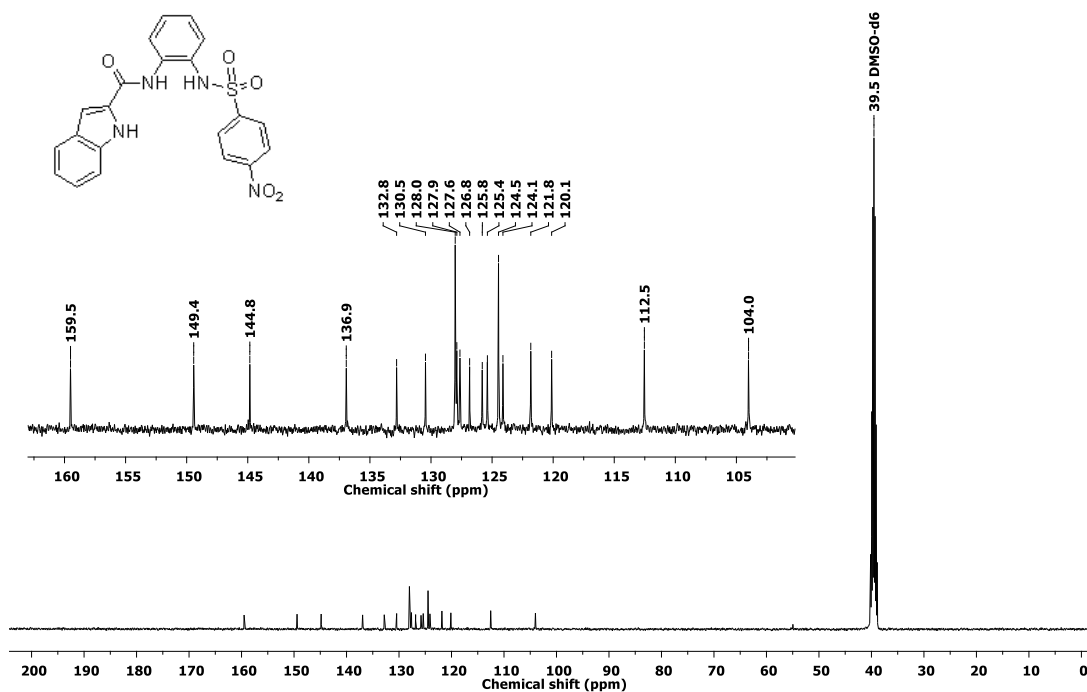

Fig. S11 ^{13}C NMR spectrum of *N*-(2-((4-nitrophenyl)sulfonamido)phenyl)-1*H*-indole-2-carboxamide **1c**.
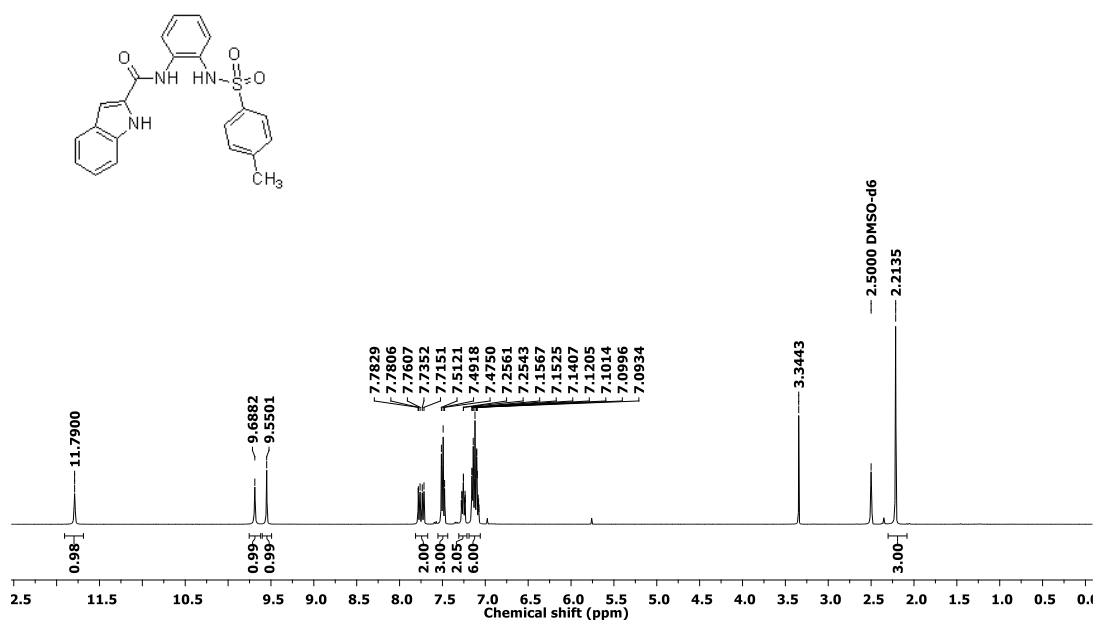
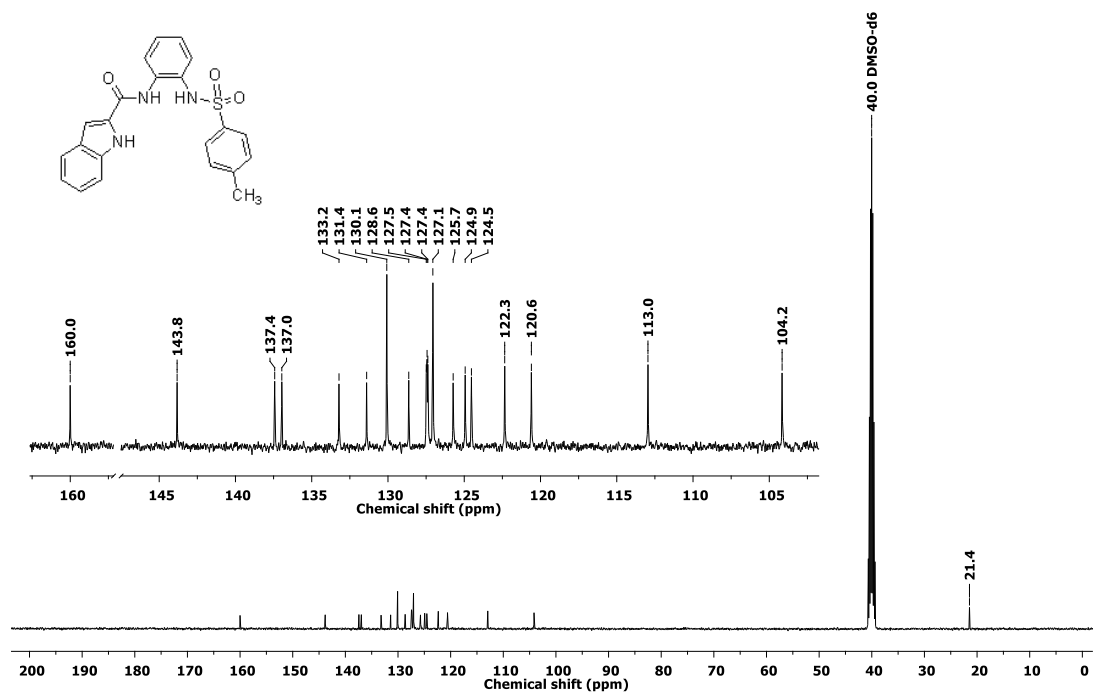**Fig. S12** ¹H NMR spectrum of *N*-(2-((4-methylphenyl)sulfonamido)phenyl)-1*H*-indole-2-carboxamide **1d**.

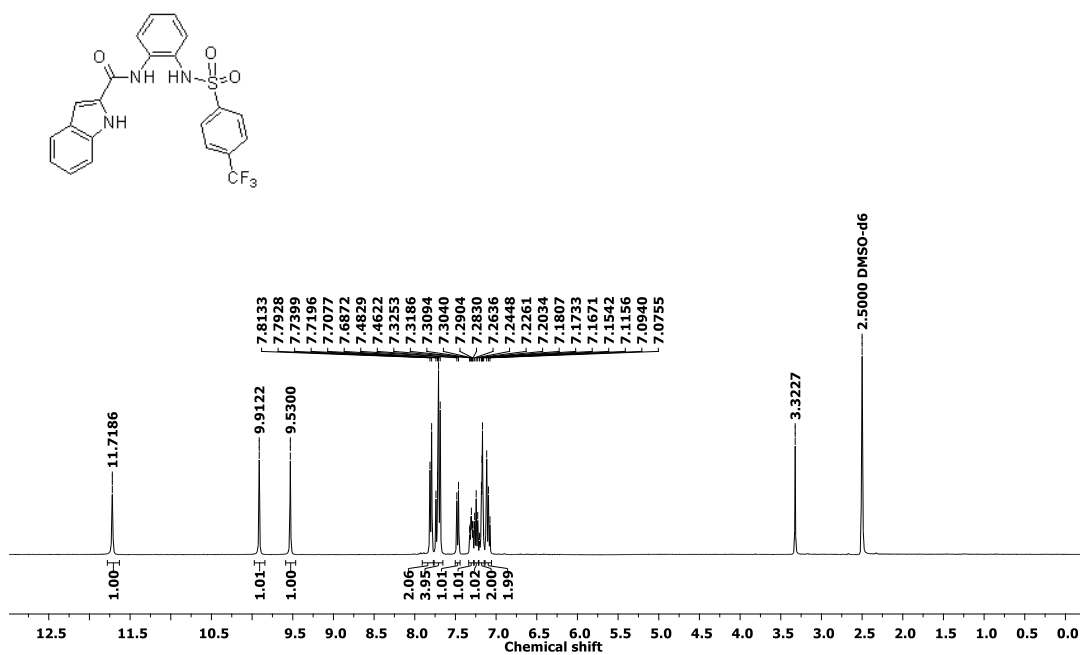**Fig. S13** ¹³C NMR spectrum of *N*-(2-((4-methylphenyl)sulfonamido)phenyl)-1*H*-indole-2-carboxamide **1d**.

S13

Fig. S14 ^{1}H NMR spectrum of *N*-(2-((4-(trifluoromethyl)phenyl)sulfonamido)phenyl)-1*H*-indole-2-carboxamide **1e**.
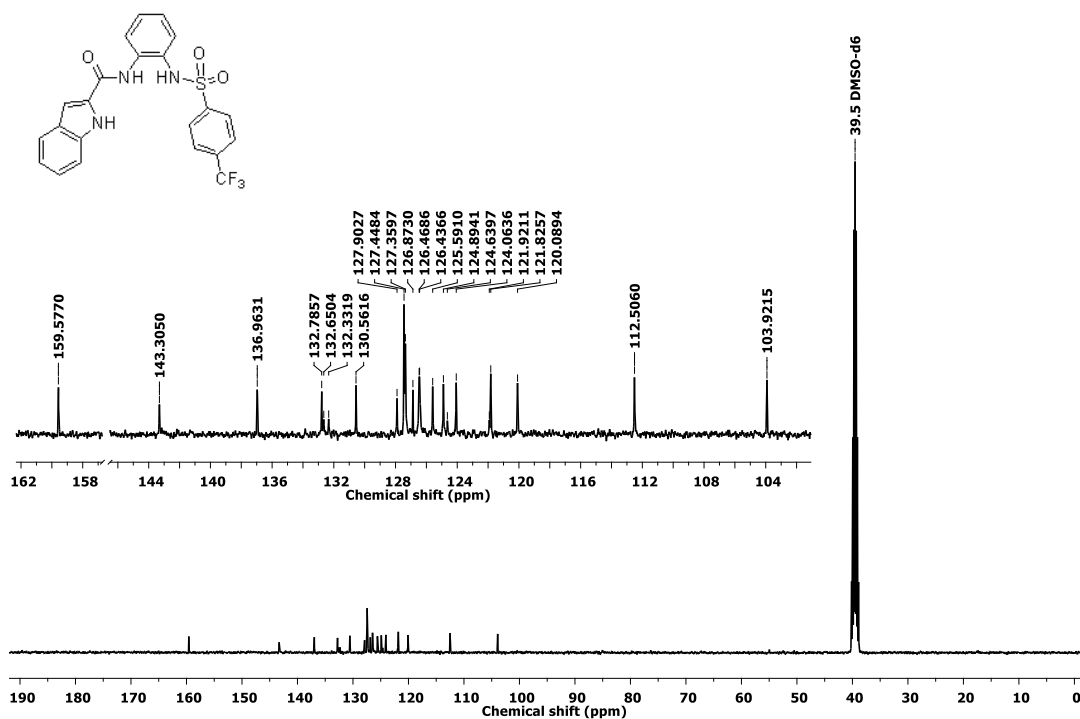

Fig. S15 ^{13}C NMR spectrum of *N*-(2-((4-(trifluoromethyl)phenyl)sulfonamido)phenyl)-1*H*-indole-2-carboxamide **1e**.
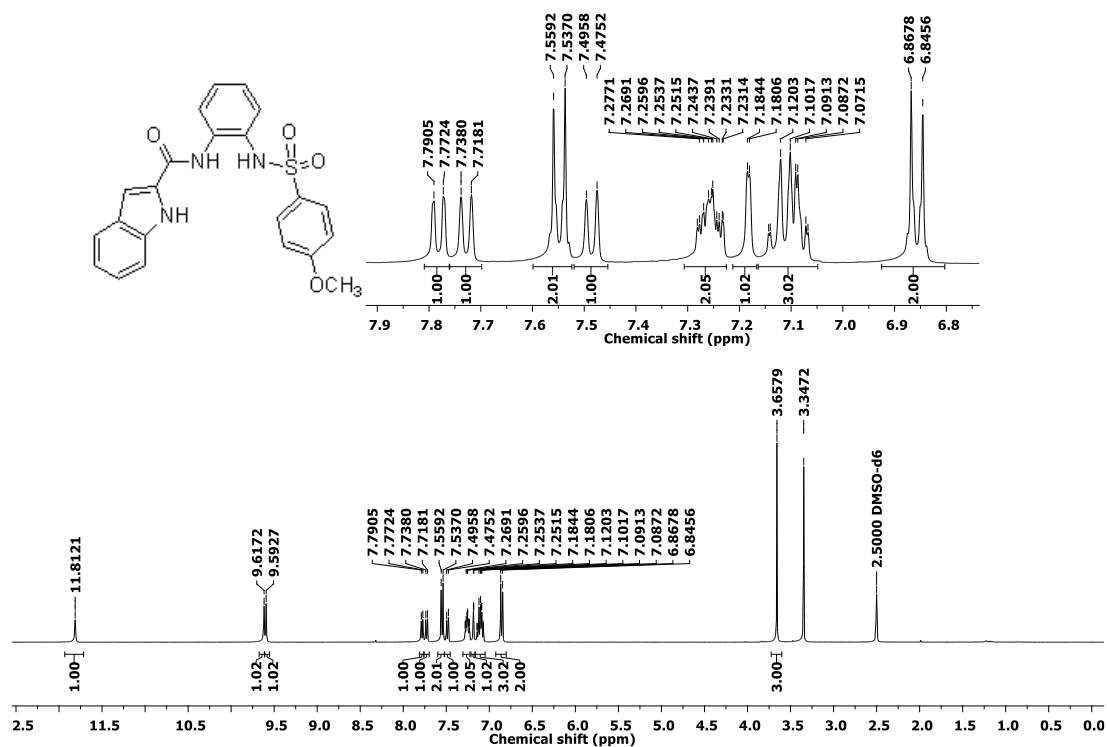
Fig. S16 ^{1}H NMR spectrum of *N*-(2-((4-methoxyphenyl)sulfonamido)phenyl)-1*H*-indole-2-carboxamide **1f**.
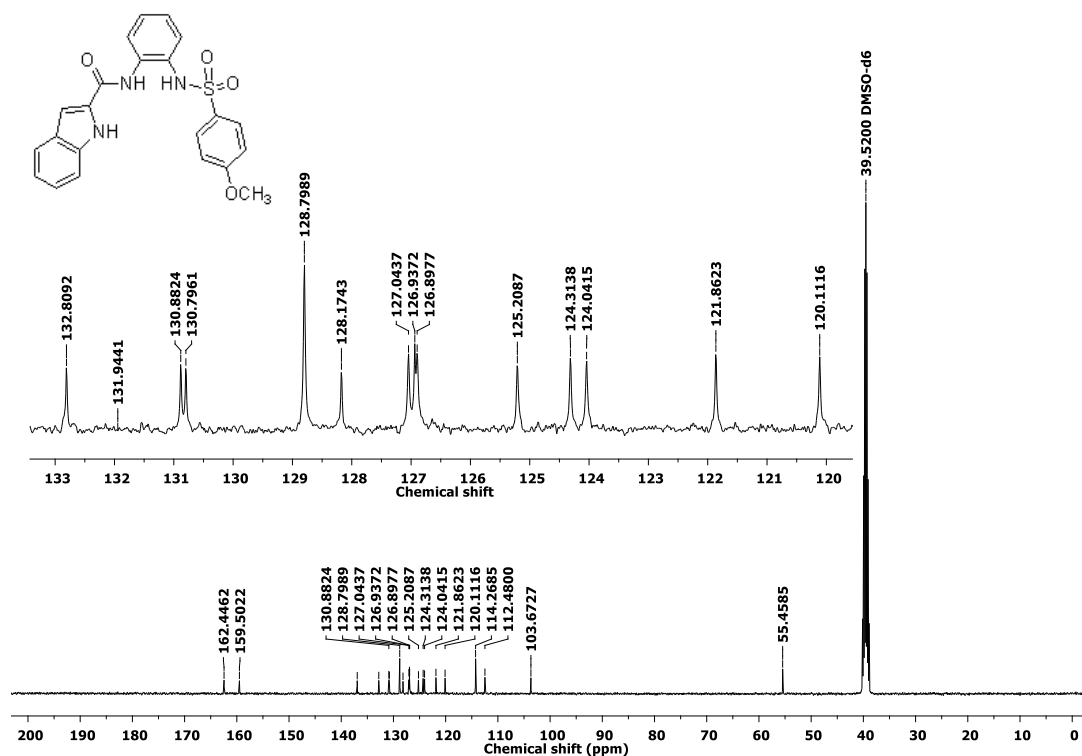

Fig. S17 ^{13}C NMR spectrum of *N*-(2-((4-methoxyphenyl)sulfonamido)phenyl)-1*H*-indole-2-carboxamide **1f**.
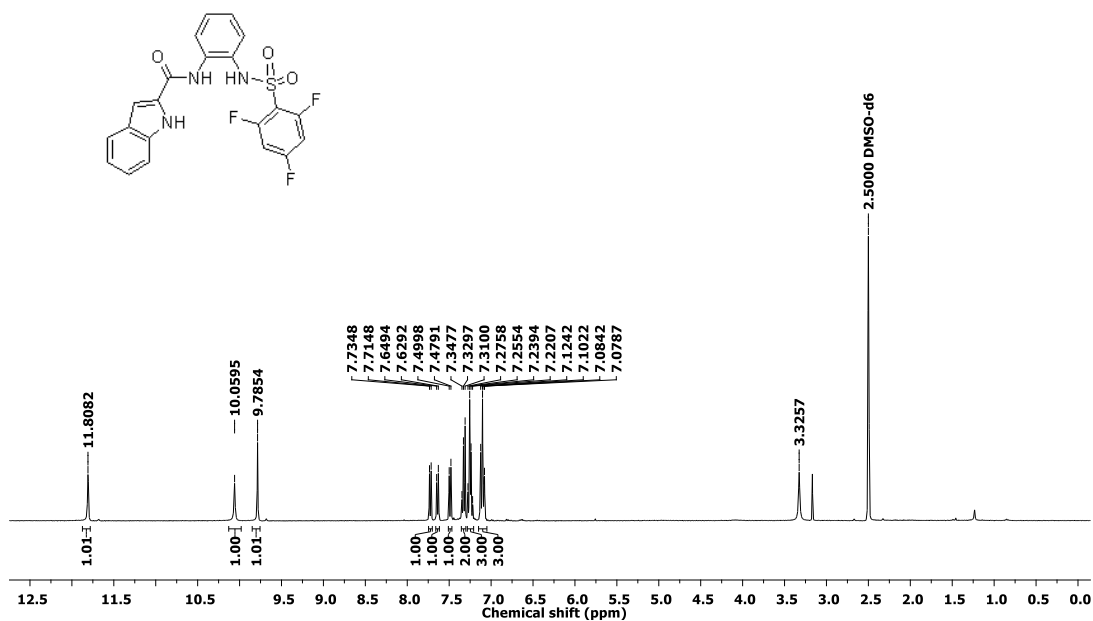
Fig. S18 ^{1}H NMR spectrum of *N*-(2-((2,4,6-trifluorophenyl)sulfonamido)phenyl)-1*H*-indole-2-carboxamide **1g**.

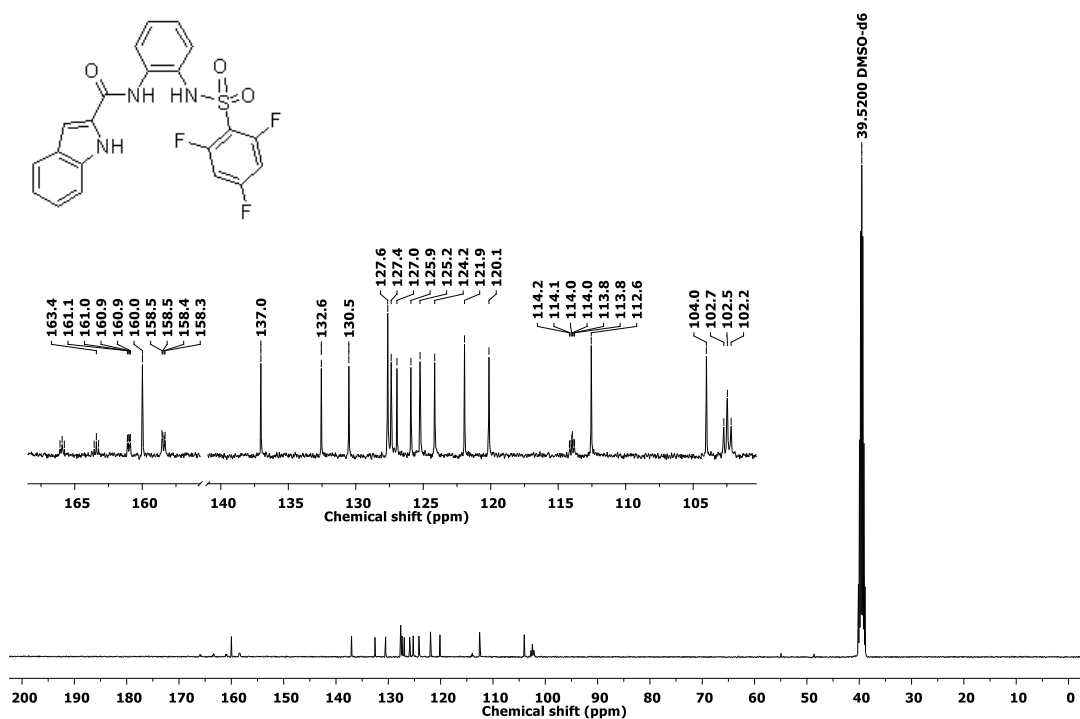**Fig. S19** ^{13}C NMR spectrum of *N*-(2-((2,4,6-trifluorophenyl)sulfonamido)phenyl)-1*H*-indole-2-carboxamide **1g**.

SV.   Single Crystal X-ray Crystallographic Analysis Study.

Single crystals suitable for X-ray diffraction were obtained by slow diffusion of atmospheric moisture into DMSO solutions of compound **1c** and **1g.** The co-crystal of [**1e·Cl⁻**][TBA⁺] was obtained by mixing the **1e** and TBACl (10 equvi.) in acetonitrile at room temperature and slow evaporation of acetonitrile gave the uniform crystals. The solid-state structure of both **1c** and **1g** showed hydrogen bonding interactions with DMSO through amide and sulfonamide N–H and indolic C–H protons (Fig. S20).

Single crystal X-ray intensity data of compounds were collected on a Bruker- KAPPA APEX II CCD diffractometer with graphite-monochromatized (Mo-Kα = 0.71073 Å) radiation. The X-ray generator was operated at 1500 W power, 50 kV and 30 mA. Data were collected with the scan width of 0.3° at different settings of φ (0°, 90° and 180°) keeping the sample to detector distance fixed at 40 mm and the detector position (2θ) fixed at 24°. The X-ray data collection was monitored by SMART program (Bruker, 2003). The structure was solved by the direct method using SHELXTL and refined on *F2* by full-matrix least squares technique using the SHELXL-974 program package within the WINGX programme. All non-hydrogen atoms were refined anisotropically. All the hydrogen atoms were placed in geometrically idealized position as riding over their parent atoms.

Details of Co-crystal of 1c·DMSO: CCDC 1840631, $C_{23}H_{22}N_4O_6S_2$, M = 514.56, colorless blocks, triclinic, space group: P -1, Cell: a=7.567(2), b=12.628(4), c=12.890(4), V = 1178.3(6) Å^3, Z = 2, , T = 296 K, θ_{max} = 28.365°, D$_{calc}$ (g cm^{-3}) = 1.450, F(000) = 536.0, μ (mm^{-1}) = 0.274, 21482 reflections collected, 5854 unique reflections (R$_{int}$ = 0.0706), GoF = 0.980, R$_1$ = 0.0554, wR$_2$ = 0.1611, R indices based on 5033 reflections with I >2s(I) (refinement on F2). $\Delta\rho_{max}$ = 0.792, $\Delta\rho_{min}$ = − 0.752 (eA^{-3}).
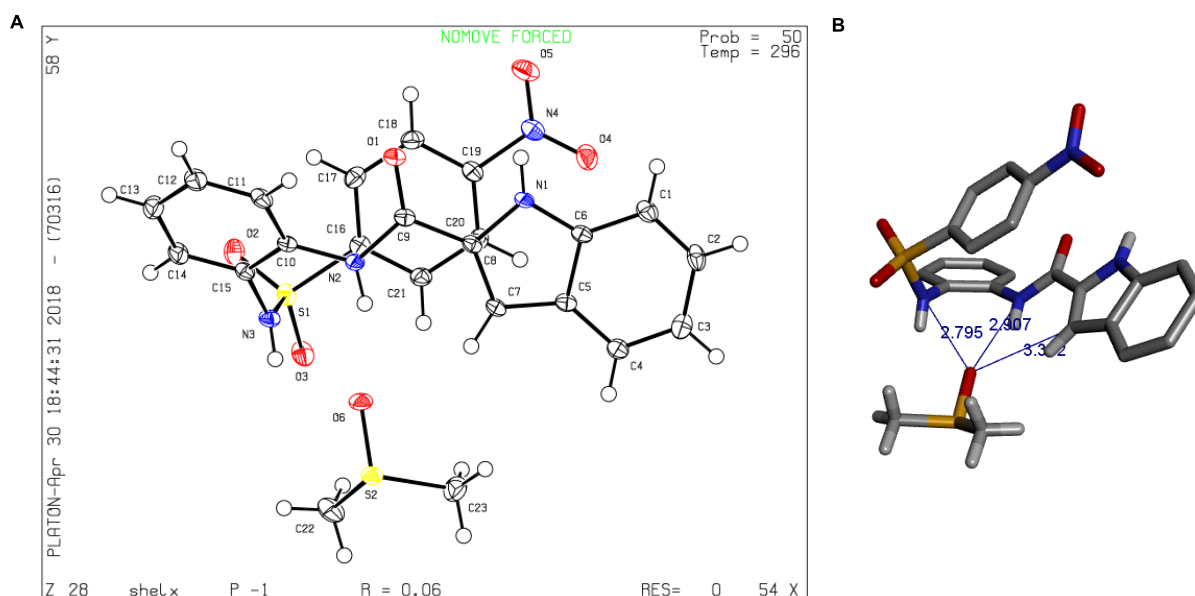

Fig. S20 ORTEP diagram (**A**) and X-ray crystal structure of [**1c·DMSO**]. For clarity, the only hydrogen atoms involved in hydrogen bonding are shown. The hydrogen bonds are shown by purple lines.

Details of Co-crystal of 1g·DMSO: CCDC 1835297, $C_{25}H_{26}F_3N_3O_5S_3$, M = 601.67, colorless blocks, Monoclinic, space group P 2_1/c, Cell: a = 19.508(2), b = 8.2786(10), c = 17.511(2) V = 2713.5(5) $Å^3$, Z = 4, T = 296 K, θ_{max} = 28.363°, D_{calc} (g cm^{-3}) = 1.473, F(000) = 1248, μ (mm^{-1}) = 0.335, 45772 reflections collected, 6778 unique reflections (R_{int} = 0.0685), GoF = 0.905, R_1 = 0.0407, wR_2 = 0.1387, R indices based on 5033 reflections with I >2s(I) (refinement on F2). $\Delta\rho_{max}$ = 0.544, $\Delta\rho_{min}$ = − 0.507 (eA^{-3}).
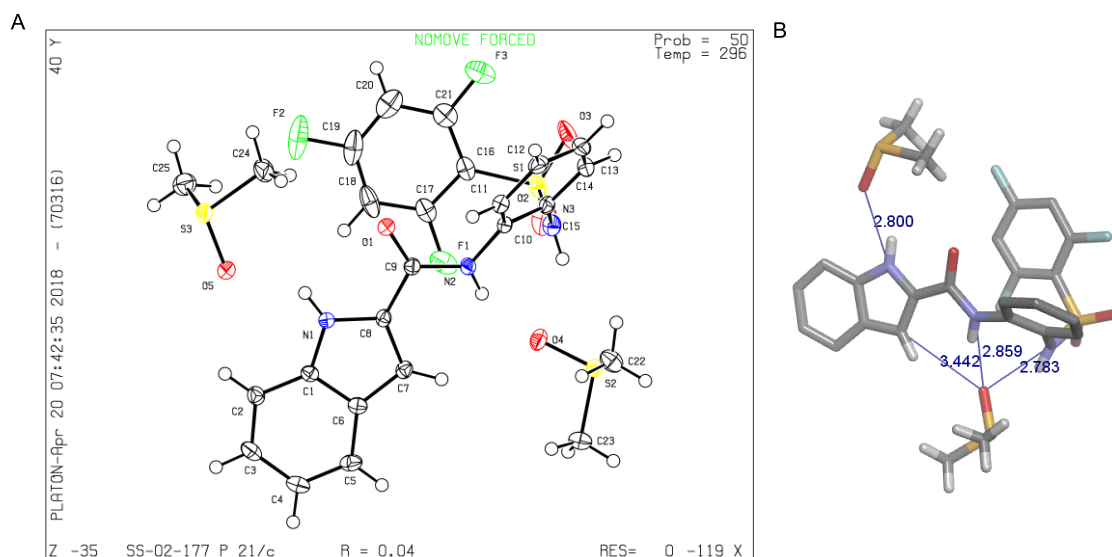

Fig. S21 ORTEP diagram (**A**) and X-ray crystal structure of [**1g**·DMSO]. For clarity, the only hydrogen atoms involved in hydrogen bonding are shown. The hydrogen bonds are shown by purple lines.

Details of co-crystal of 1e with TBACl: CCDC 1838526, $C_{38}H_{52}ClF_3N_4O_{4.5}S$, M = 761.34, colorless blocks, Monoclinic, space group C2/c, Cell: a = 20.234(4), b = 13.246(2), c = 30.365(6) V = 7963(2) $Å^3$, Z = 8, , T = 296 K, θ_{max} = 25.086°, D_{calc} (g cm^{-3}) = 1.270, F(000) = 3232, μ (mm^{-1}) = 0.207, 38339 reflections collected, 7067 unique reflections (R_{int} = 0.0625), GoF = 1.031, R_1 = 0.0888, wR_2 = 0.2830, R indices based on 4668 reflections with I >2s(I) (refinement on F2). $\Delta\rho_{max}$ = 0.947, $\Delta\rho_{min}$ = − 0.640 (eA^{-3}).
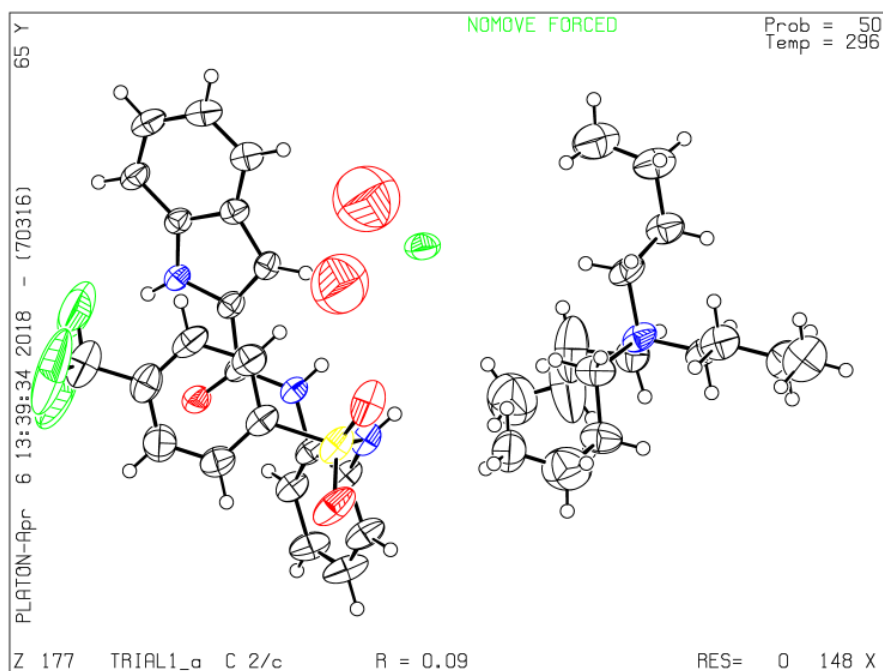
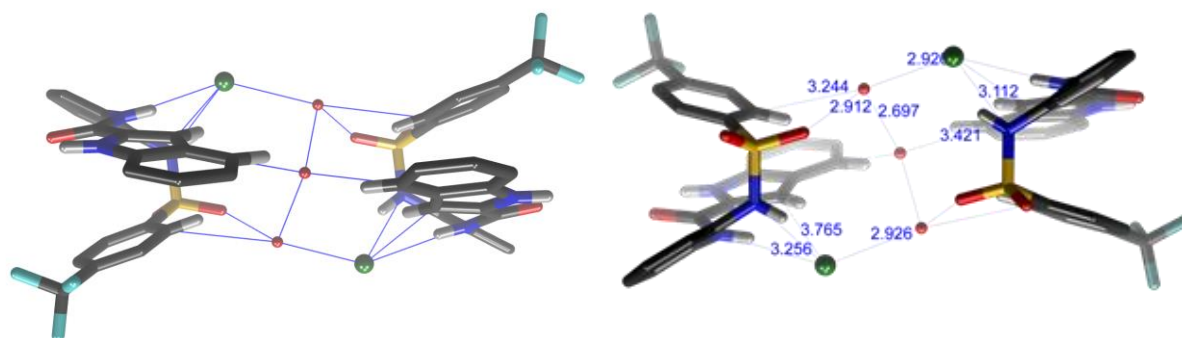**Fig. S22A** ORTEP diagram of **1e** co-crystalized with TBACl.

Fig. S22B Front and back view of co-crystal of **1e·Cl⁻**.

Hirshfeld Surface Analysis:

The Hirshfeld surface analysis is very useful tool to identify the intermolecular interactions in molecular crystals. The tool has been widely used for analyzing the interactions in crystal structures.[S3,S4] This tool also provide the C-H···X (X = N, O, Cl, etc.). The presences of hydrogen bonding interactions were visualized using the CrystalExplorer-17.5 software. The results of Hirshfeld surface analysis shown in the Fig. 23. The program was used to identified the C(H)···Cl⁻ and C(H)···O contacts as hydrogen bonds (see Fig. S23A). To understand the electron density distribution on the receptor molecule in co-crystal structure using the CrystalExplorer-17.5 program.[S2] The Hirshfeld surface was also generated for the Cl⁻ ions in the same software (Fig. 23B). The red, white, blue and color code indicates strong, medium and weak interactions respectively.[S4,S5] The results obtained are analogous to the previously predicted results obtained using Mercury 3.0 software. We have also generated the electrostatic potential of the receptor using the crystal data. The electrostatic potential on

receptor surface generated in crystalExplorer17 software using the default program "Tonto", method "DFT" and basis set "6-31G(d)" (Fig. 1D). In this case, the blue and red colors indicate the electron deficient and electron rich areas on a molecule (Fig. 2D). The analysis clearly indicates that the indole NH, carboxyamide NH and sulfonamide NH are strongly electron deficient while three CH protons (H_a, H_c and H_e) are moderately electron deficient. Therefore, these centers can participate in hydrogen bonds.
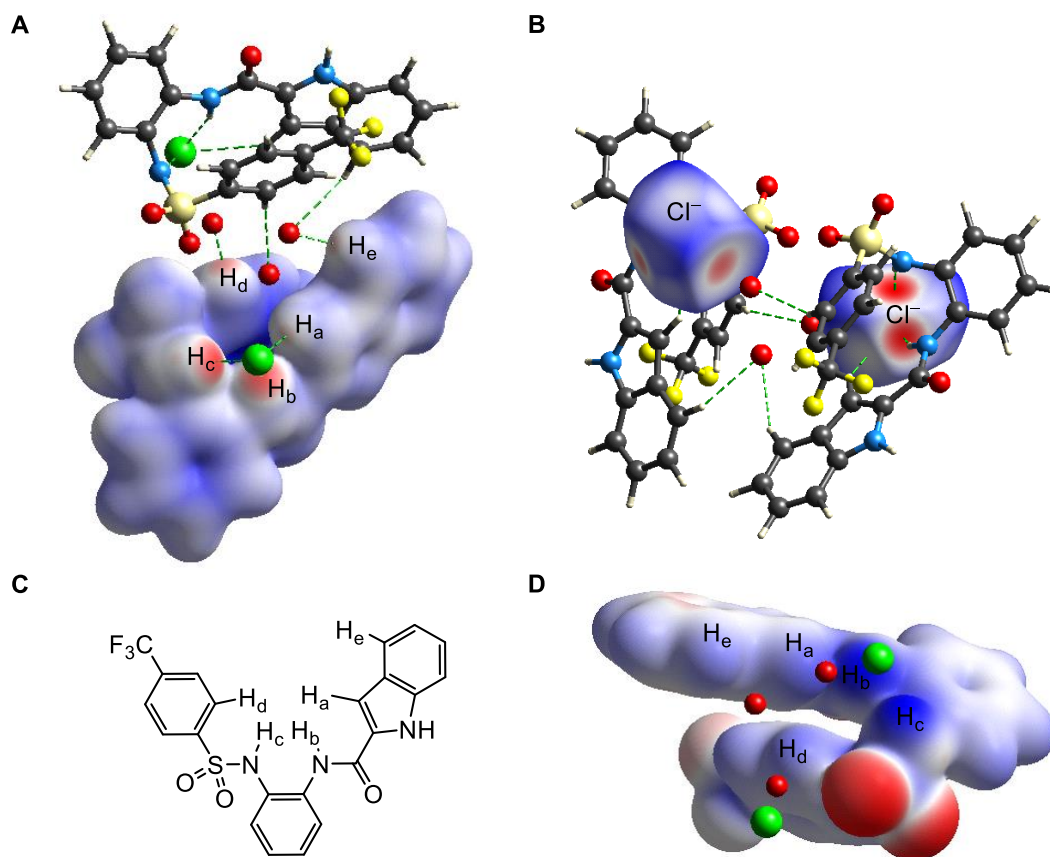

Fig. S23. The d$_{norm}$ mapped over the Hirshfeld surface using universal red, blue and white color code to show important interactions taking a neighbouring molecule. Hirshfeld surface generated for receptor (**A**) and Cl$^-$ atoms (**B**). The red, white, blue and color code indicates strong, medium and weak interactions respectively. The ChemDraw structure of receptor **1e** (**C**). The electrostatic potential on receptor surface generated in *crystalExplorer17* software using the default program "Tonto", method "DFT" and basis set 6-31G(d) (**D**). In electrostatic potential surface the blue and red colors indicate the electron deficient and electron rich areas on a molecule.

SVI. ^{1}H NMR Binding Studies

The stock solutions of **1a-1g** (0.01M) and tetrabutylammonium chloride (1M) were prepared in either acetonitrile-d_3 or DMSO-d_6. All the receptors and TBACl were dried in vacuum desiccator before use. ^{1}H NMR spectra were recorded on a Bruker Ascent^{TM} 400 spectrometer and calibrated with respect to residual protic solvent peak in Acetonitrile-d_6 (δ = 1.94). NMR titrations were performed by successive addition of aliquots of the apparent anionic guest as

the tetrabutylammonium (TBA) salt. In acetonitrile-d_6, a change in the chemical shift of all three NH (Amide NH, indole NH, and Sulfonamide NH) was observed. The ^{1}H NMR stacked plots were processed using MestReNova 6 software. To obtain the binding constants data was curve fitted with 1:1 binding model of the WinEQNMR2 computer program[S6]
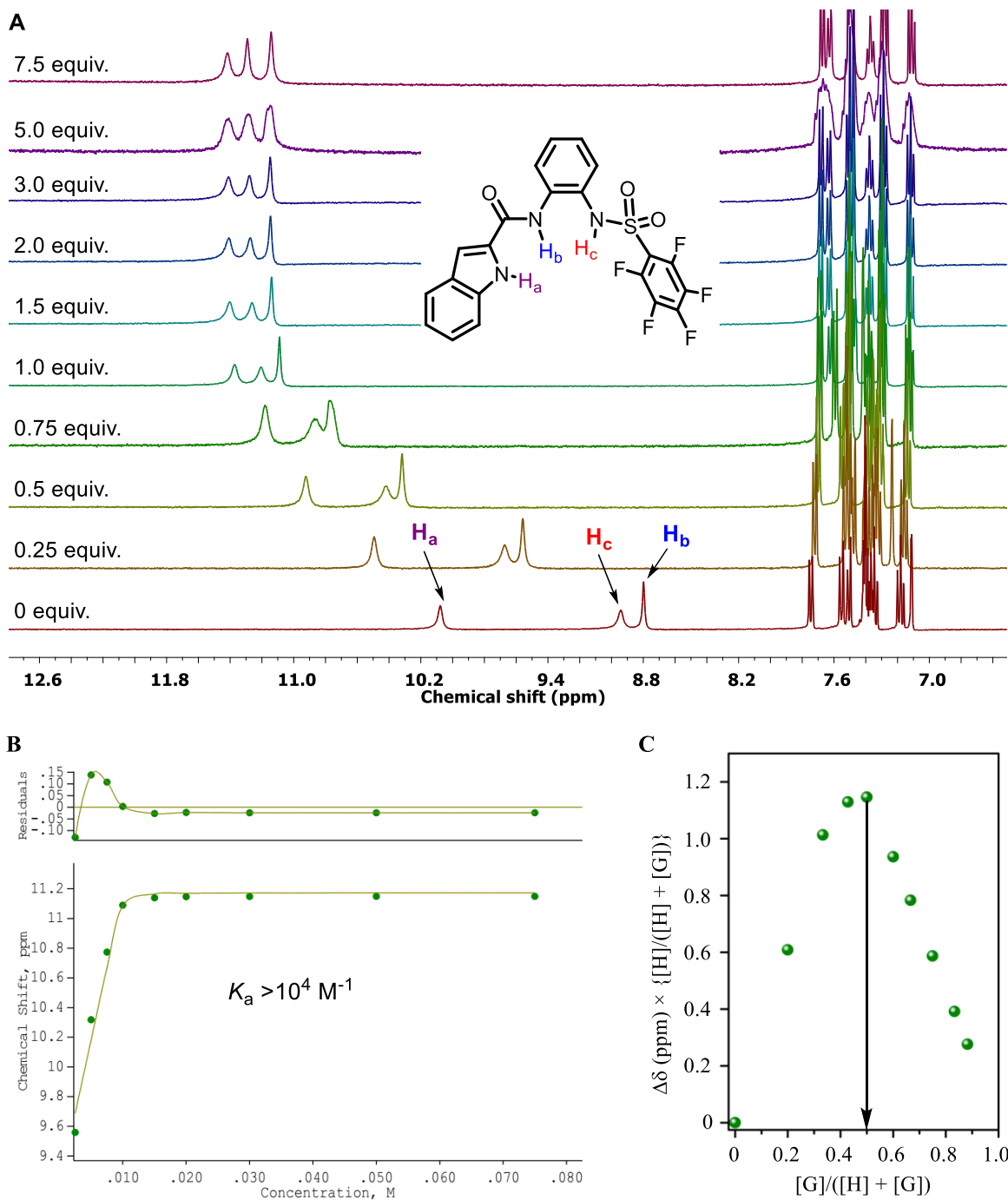
Fig. S24 ^{1}H NMR titration spectra for **1a** with stepwise addition of TBACl in acetonitrile-d_3 at 25 °C. The equivalents of added TBACl are shown on the stacked spectra (**A**). Fit plot of chemical shift (δ ppm) of sulfonamide NH proton versus concentration of TBACl fitted to 1:1 binding model of WinEQNMR2 program (**B**). Job's plot generated from the same ^{1}H NMR titration indicating 1:1 binding of **1a**:Cl⁻ (**C**).
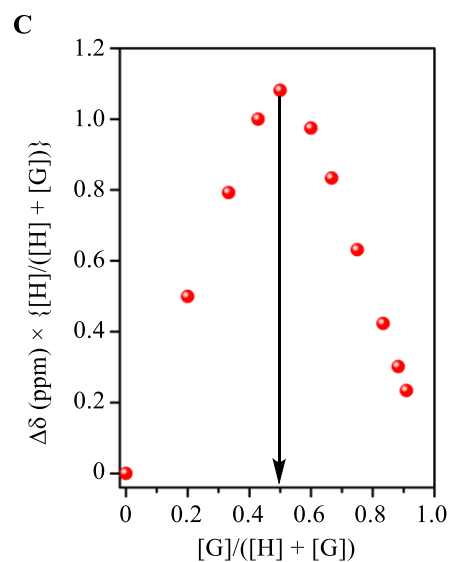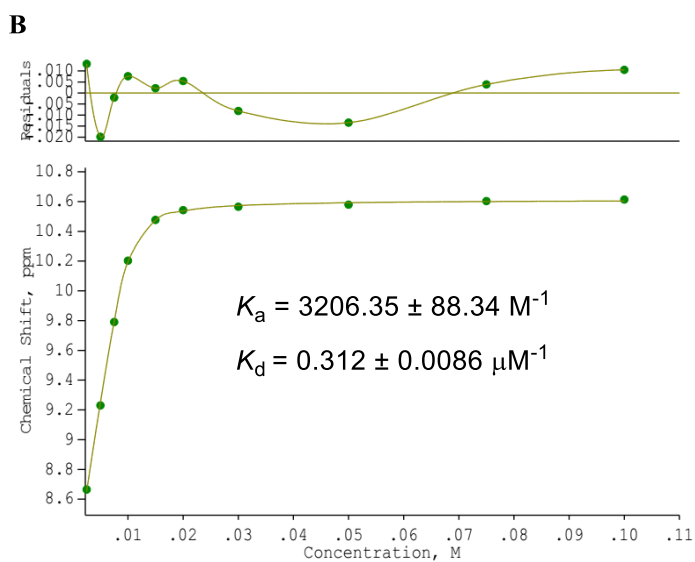
Fig. S25 ^{1}H NMR titration spectra for **1d** with stepwise addition of TBACl in acetonitrile-d_3 at 25 °C. The equivalents of added TBACl are shown on the stacked spectra (**A**). Fit plot of chemical shift (δ ppm) of sulfonamide NH proton versus concentration of TBACl fitted to 1:1 binding model of the WinEQNMR2 program (**B**). Job's plot generated from the same ^{1}H NMR titration indicating 1:1 binding of **1d**:Cl$^-$ (**C**).
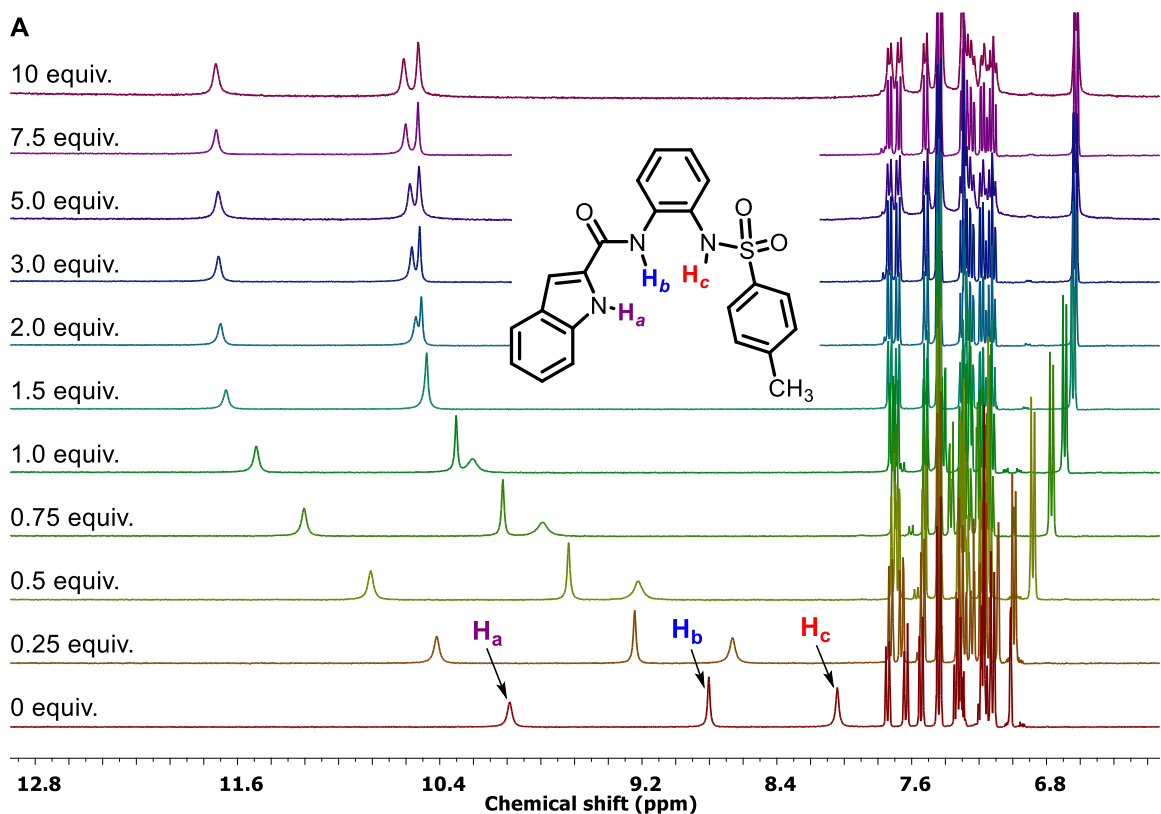
Fig. S26 ^{1}H NMR titration spectra for **1e** with stepwise addition of TBACl in acetonitrile-d_3 at 25 °C. The equivalents of added TBACl are shown on the stacked spectra (**A**). Fit plot of chemical shift (δ ppm) of sulfonamide NH proton versus concentration of TBACl fitted to 1:1 binding model of WinEQNMR2 program (**B**). Job's plot generated from the same ^{1}H NMR titration indicating 1:1 binding of **1e**:Cl⁻ (**C**).
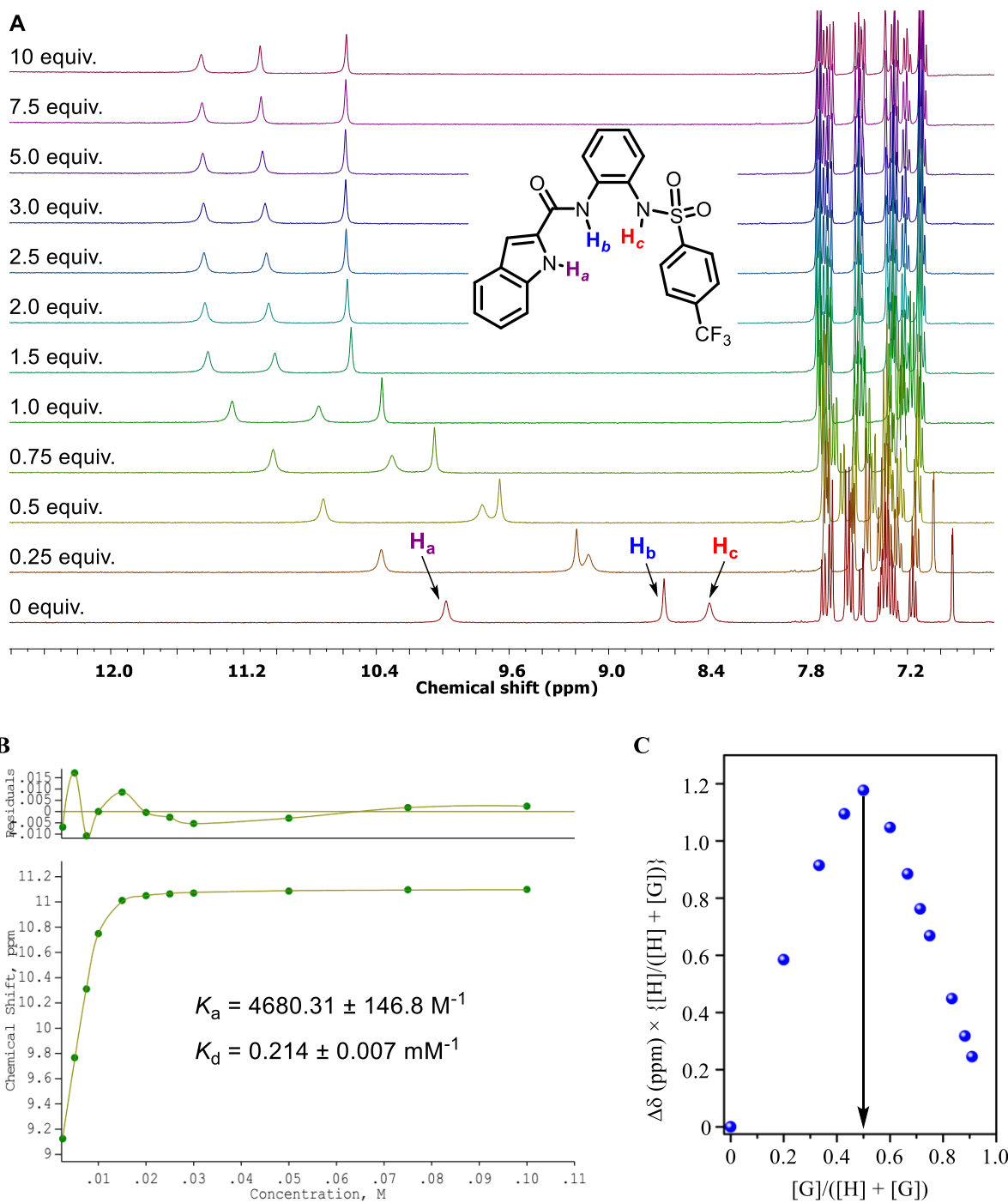
Fig. S27 ^{1}H NMR titration spectra for **1f** with stepwise addition of TBACl in acetonitrile-d_3 at 25 °C. The equivalents of added TBACl are shown on the stacked spectra (**A**). Fit plot of chemical shift (δ ppm) of sulfonamide NH proton versus concentration of TBACl fitted to 1:1 binding model of WinEQNMR2 program (**B**). Job's plot generated from the same ^{1}H NMR titration indicating 1:1 binding of **1f**:Cl⁻ (**C**).
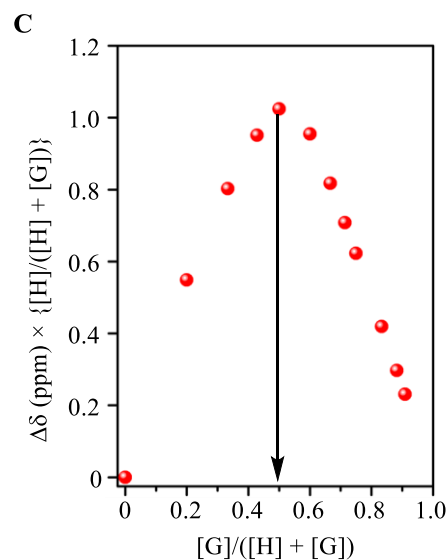
Fig. S28 ^{1}H NMR titration spectra for **1g** with stepwise addition of TBACl in acetonitrile-d_3 at 25 °C. The equivalents of added TBACl are shown on the stacked spectra (**A**). Fit plot of chemical shift (δ ppm) of sulfonamide NH proton versus concentration of TBACl fitted to 1:1 binding model of WinEQNMR2 program (**B**). Job's plot generated from the same ^{1}H NMR titration indicating 1:1 binding of **1g**:Cl⁻ (**C**).
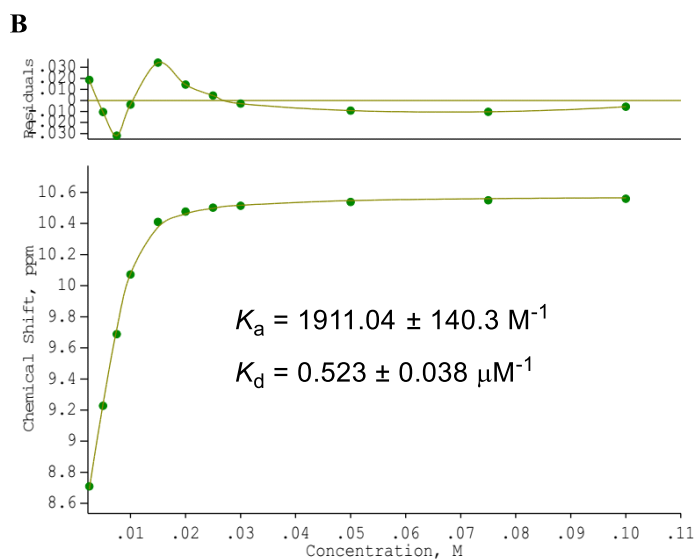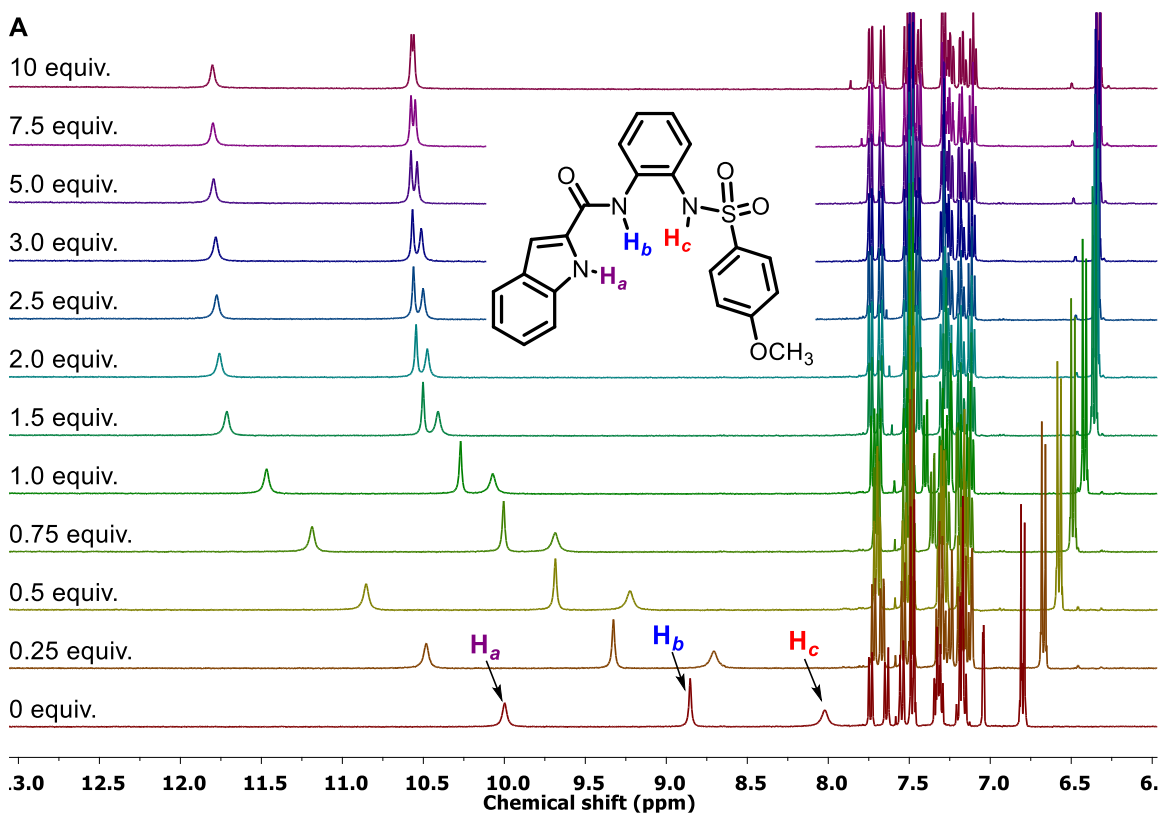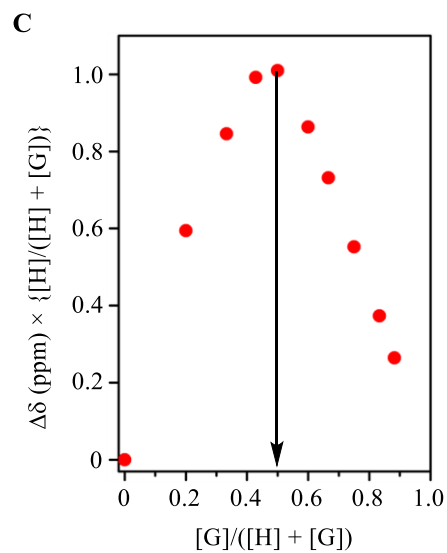
Fig. S29 ^{1}H NMR titration spectra for **1d** with stepwise addition of TBABr in acetonitrile-d_3 at 25 °C. The equivalents of added TBABr are shown on the stacked spectra (**A**). Fit plot of chemical shift (δ ppm) of sulfonamide NH proton versus concentration of TBABr fitted to 1:1 binding model of WinEQNMR2 program (**B**)
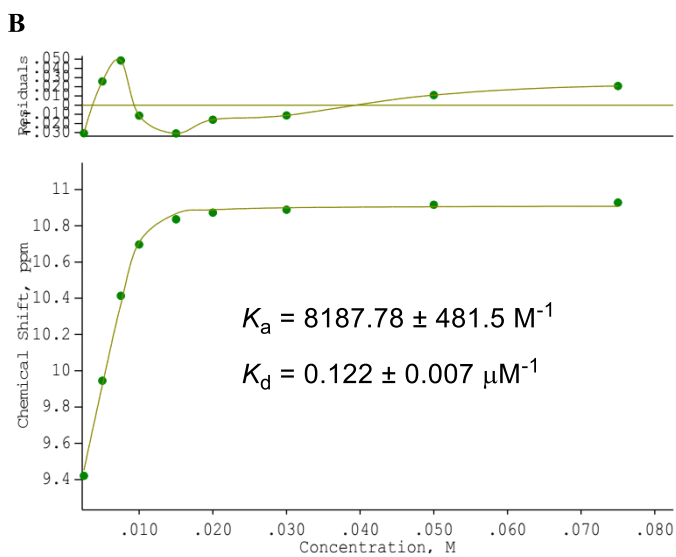
Fig. S30 ^{1}H NMR titration spectra for **1d** with stepwise addition of TBAI in acetonitrile-d_3 at 25 °C. The equivalents of added TBAI are shown on the stacked spectra (**A**).
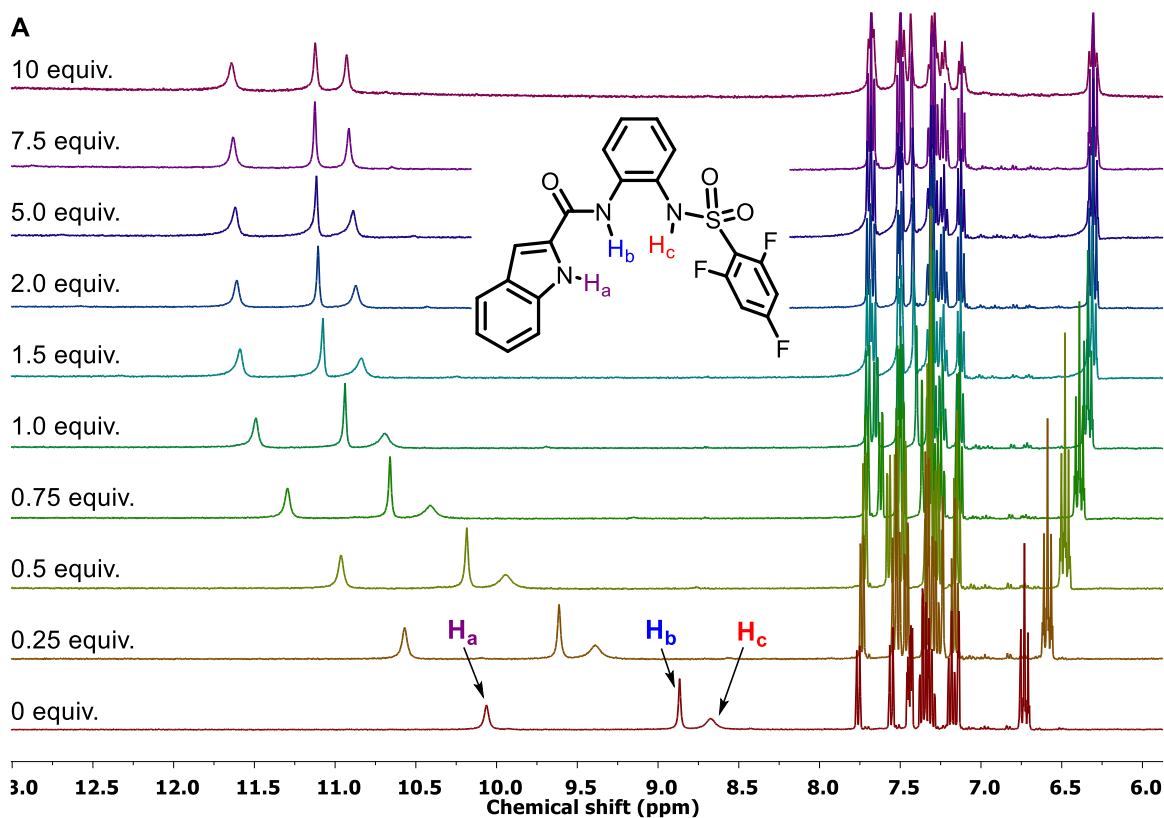

Fig S31 ^{1}H NMR titration spectra for **1d** with stepwise addition of TBAF in acetonitrile-d_3 at 25 °C. The equivalents of added TBAF are shown on the stacked spectra.

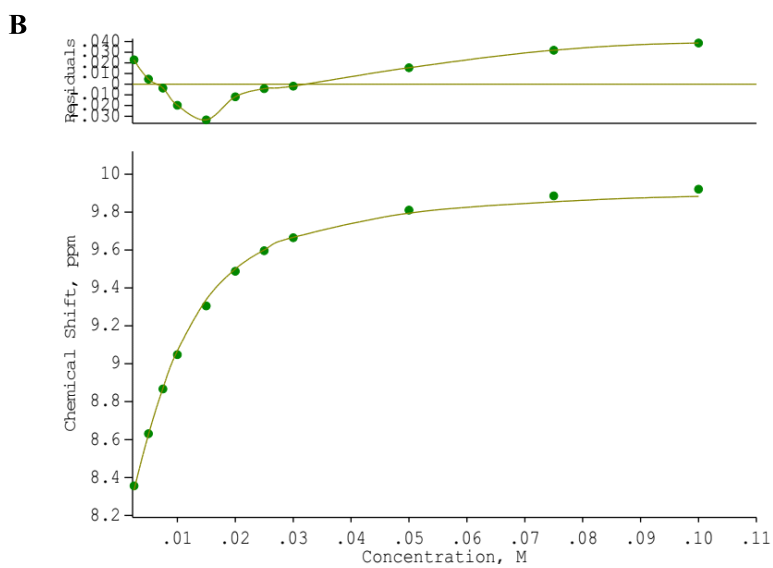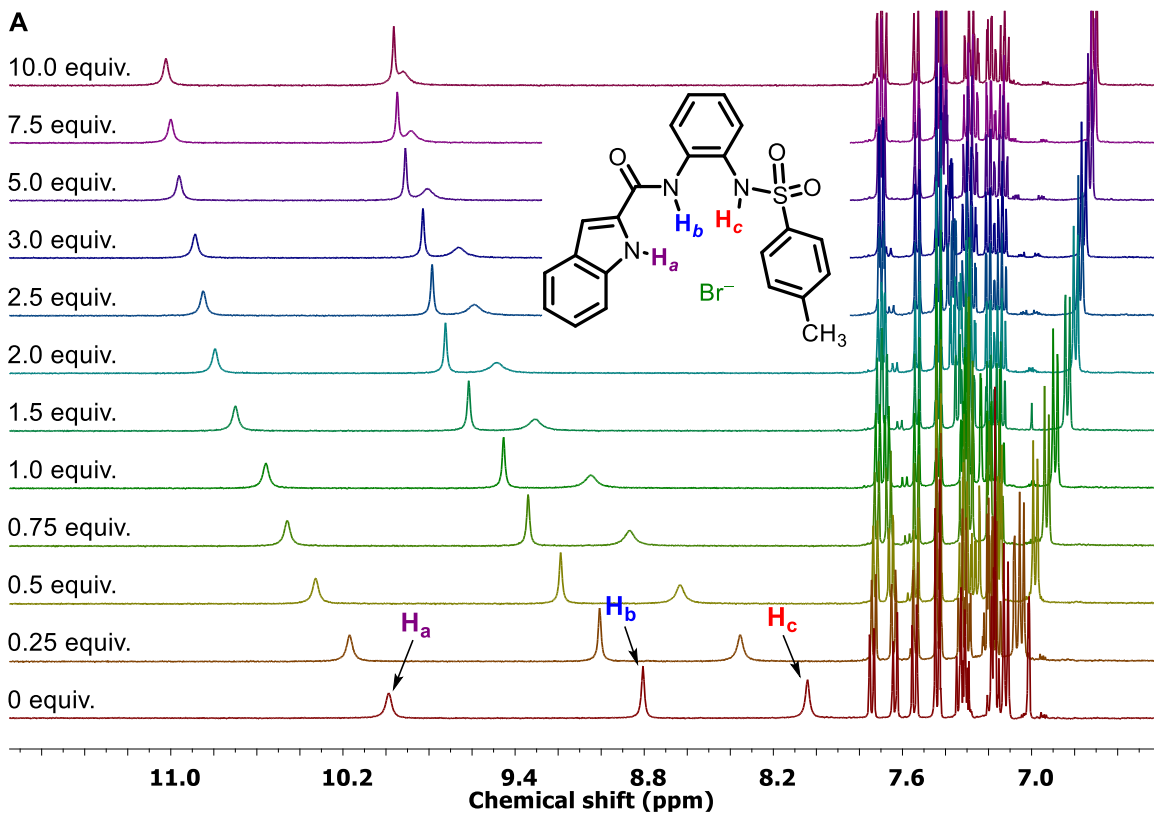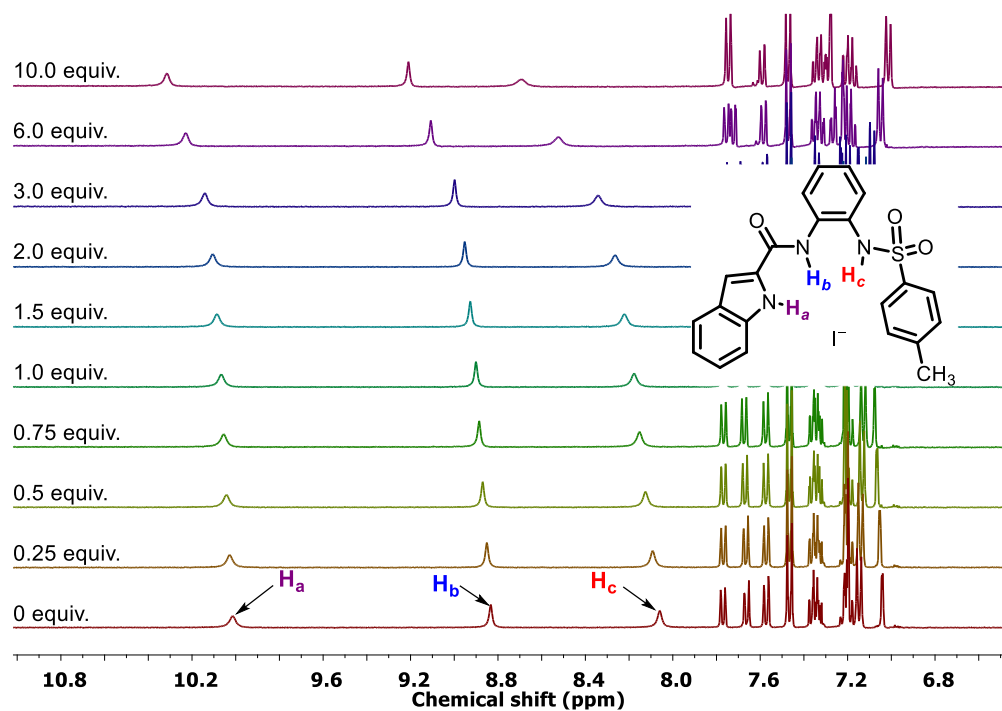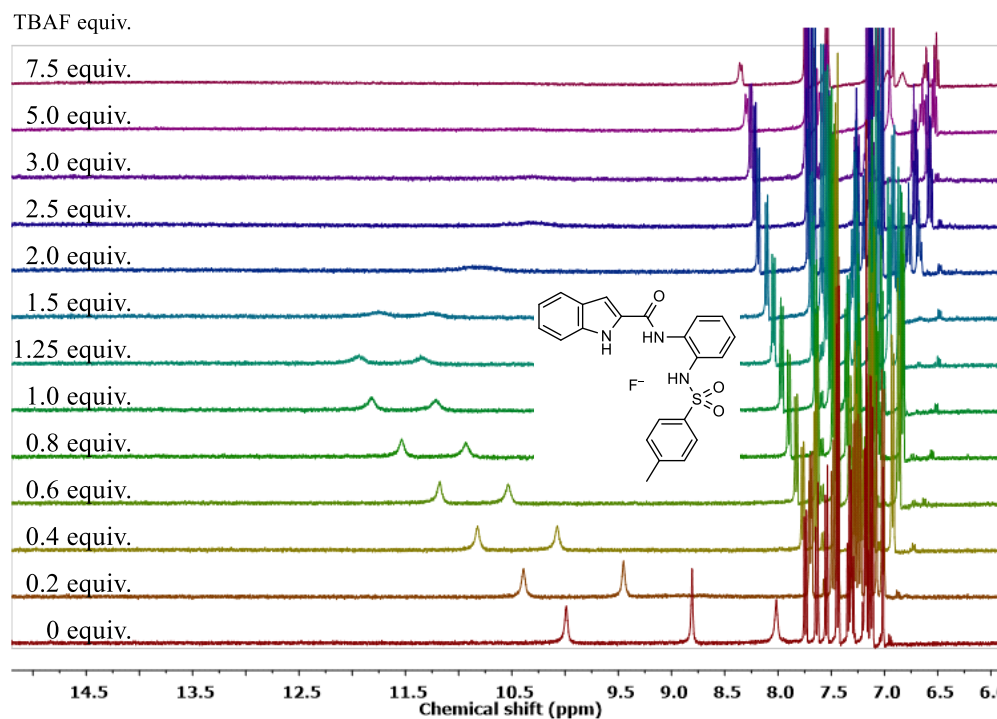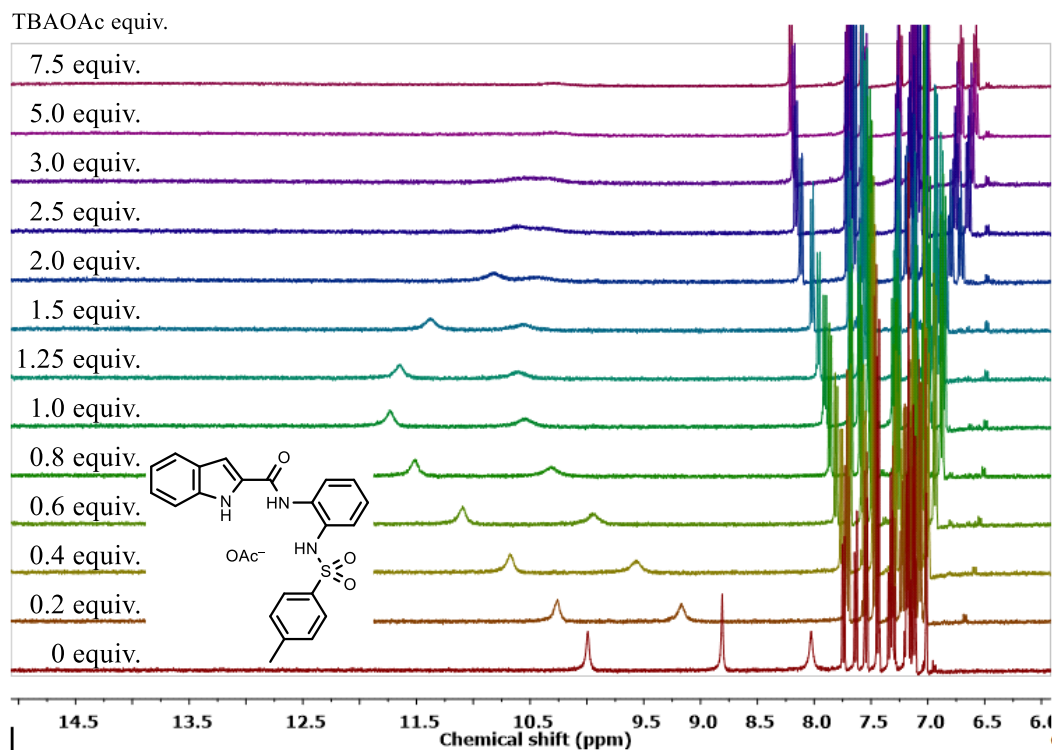**Fig S32** ^{1}H NMR titration spectra for **1d** with stepwise addition of TBAOAc (**B**) in acetonitrile-d_3 at 25 °C. The equivalents of added TBAOAc are shown on the stacked spectra.

SVII. Ion Transport Studies:

A. Preparation of EYPC-LUVs⊃HPTS in NaCl: In a 10 mL clean and dry round bottom flask a thin and transparent film of egg yolk phosphatidylcholine (EYPC) was prepared by drying 1 mL of EYPC lipid (25 mg/mL in $CHCl_3$) with continuous rotation and slow purging of nitrogen gas. The transparent film then dried in high vacuum for 5-6 hours to remove all the traces of $CHCl_3$. The dried lipid film was hydrated with 1 mL of buffer (10 mM HEPES, 100 mM NaCl, 1mM HPTS, pH = 7.0). The resulting suspension was vortexed at an interval of 10 minutes during 60 minutes. The suspension was then subjected to 10 freeze-thaw cycles (liquid N_2, 55 °C Water bath), and > 19 times (must be an odd number) extruded through a polycarbonate membrane of pore size 100 nm. An extravesicular dye was removed by size exclusion chromatography using Sephadex G-50 (Sigma-Aldrich) by eluting with buffer (10 mM HEPES, 100 mM NaCl, pH = 7.0). Finally, the vesicular suspension was diluted to 6 mL. Final conditions: ~ 5 mM EYPC; *inside*: 10 mM HEPES, 100 mM NaCl, 1 mM HPTS, pH 7.0; *outside*: 10 mM HEPES, 100 mM NaCl, pH 7.0.

B. Ion Transport Activity by HPTS Assay:[S7] In a clean and dry fluorescence cuvette, 1975 µL of buffer (10 mM HEPES, 100 mM NaCl, pH 7.0) was added followed by the addition of 25 µL EYPC-LUV⊃HPTS vesicles. The resulting solution was slowly stirred with the magnetic stirrer equipped with the fluorescence instrument. The time-dependent change in fluorescence intensity at λ_{em} = 510 nm was monitored at excitation wavelength λ_{ex} = 450 nm during the addition of base (20 µL, 0.5 M NaOH to create pH gradient) at t = 20 s, transporter molecule as DMSO solution at t = 100 s, and finally 10% Trion X-100 (25 µL) at t = 300 s was added to lyse the vesicles so that the complete destruction of pH gradient is achieved (Fig. S30A and S30B). The collected data was then normalized to the percentage change in fluorescence intensity as a course of time using the equation 1:

$$I_F = [(I_t - I_0)/(I_\infty - I_0)] \times 100 \qquad\qquad \text{(Equation 1)}$$

Where, I_0 is the initial intensity, I_t is the intensity at time t, and I_∞ is the final intensity after addition of Triton X-100.
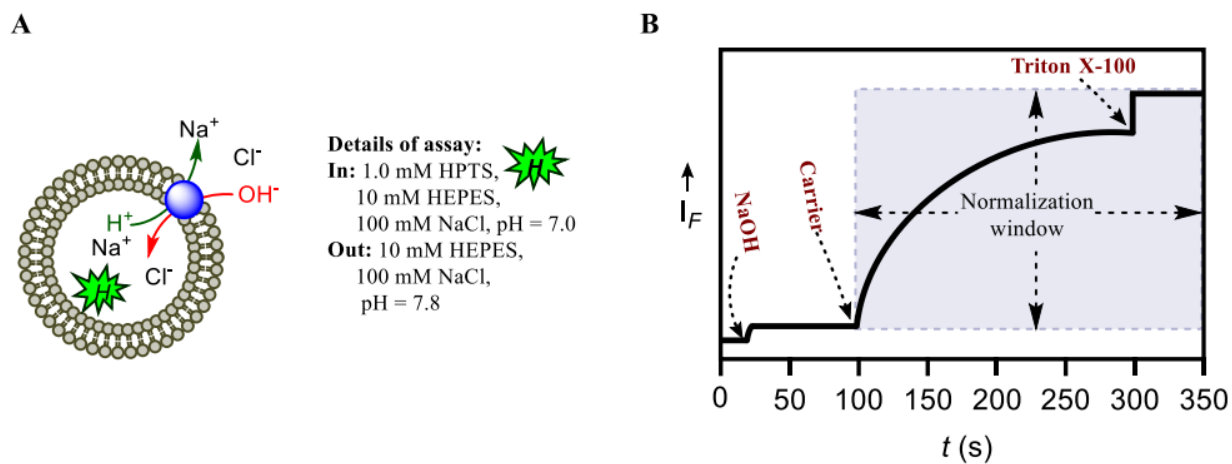
Fig. S33 Representations of fluorescence-based ion transport activity assay using EYPC-LUVs (**A**) and representative ion transport kinetics showing normalization window (**B**).

R	pK_a	LogP
p-CH$_3$	7.44	4.73
p-Br	7.28	4.99
p-CF$_3$	7.28	5.10
p-OCH$_3$	7.52	4.06
p-NO$_2$	7.01	4.16
1,2,3,4,5-Pentafluoro	5.59	4.94
2,4,6-Trifluoro	5.75	4.65
DMSO		
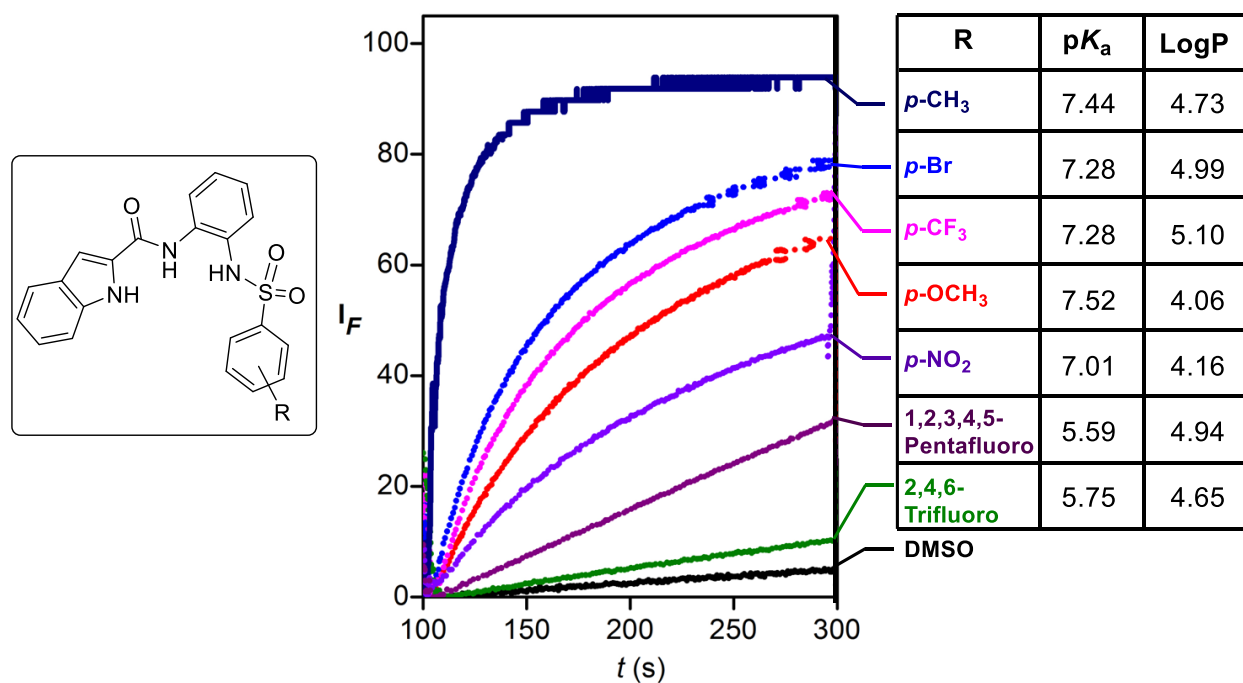
Fig. 34 Ion Transport Activity of Transporter **1a - 1g** (10 μM) across EYPC-LUVs

Fig. 35 Dose-response activity of **1b** across EYPC-LUVs⊃HPTS (**A**). Hill analysis at 250 seconds (**B**).
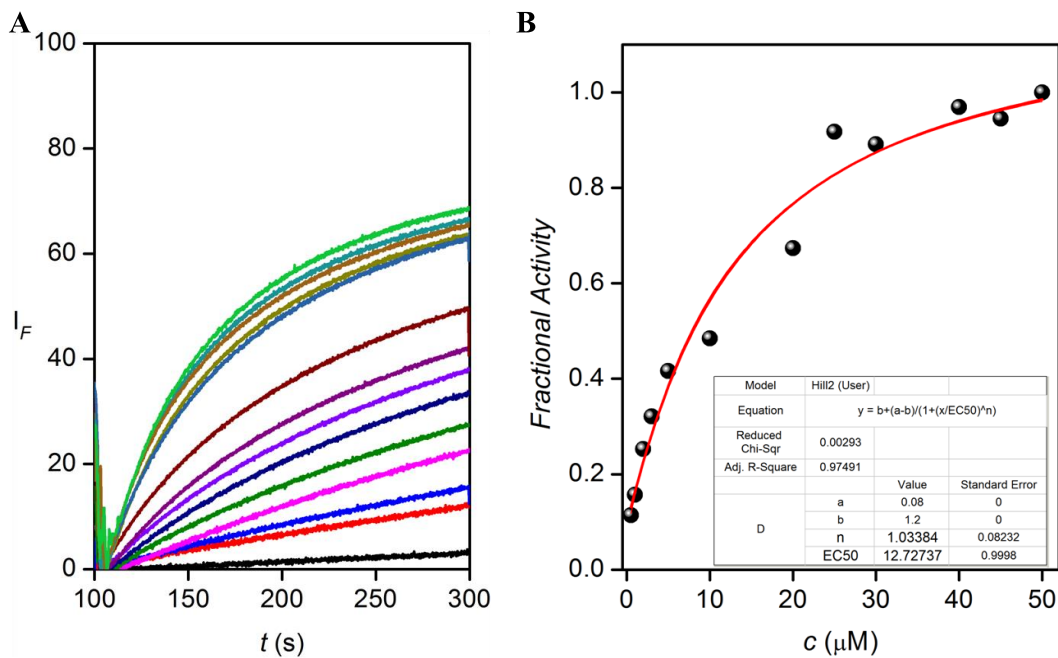
Fig. 36 Dose-response activity of **1c** across EYPC-LUVs⊃HPTS (**A**). Hill analysis at 250 seconds (**B**).

Fig. 37 Dose-response activity of **1d** across EYPC-LUVs⊃HPTS (**A**). Hill analysis at 250 seconds (**B**).

Fig. 38 Dose-response activity of **1e** across EYPC-LUVs⊃HPTS (**A**). Hill analysis at 250 seconds (**B**).

Fig. 39 Dose-response activity of **1f** across EYPC-LUVs⊃HPTS (**A**). Hill analysis at 250 seconds (**B**).

C. Preparation of EYPC-LUV⊃ANTS/DPX:

In a 10 mL round botton flask, 1 mL solutions of EYPC lipid (25 mg/mL) in CHCl3 was dried under a stream of N_2 with continuous rot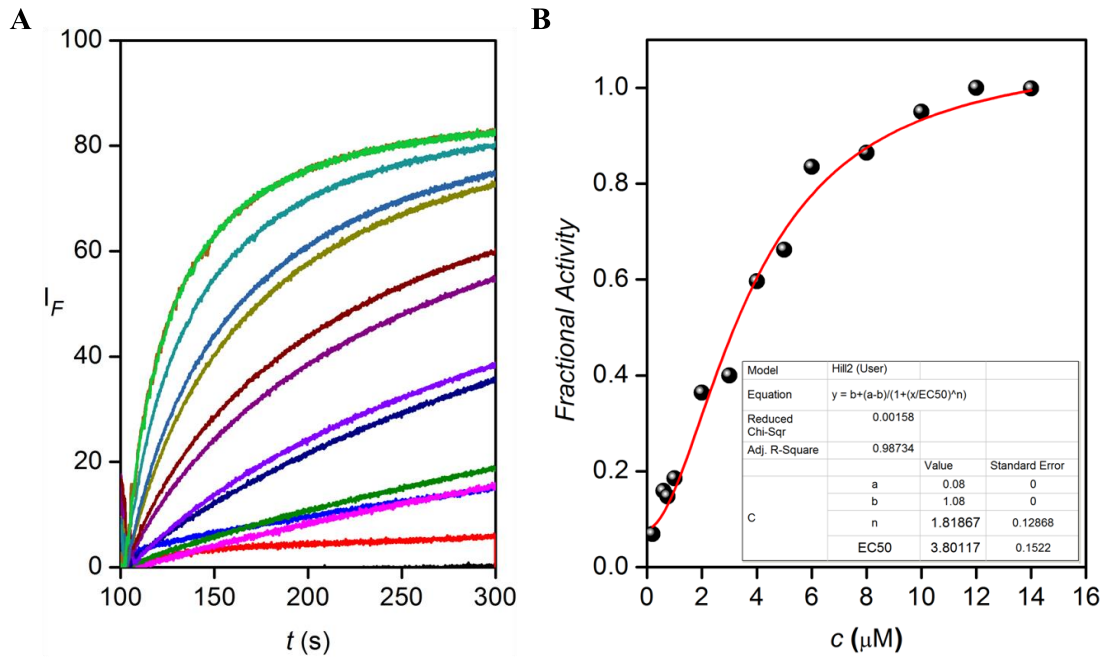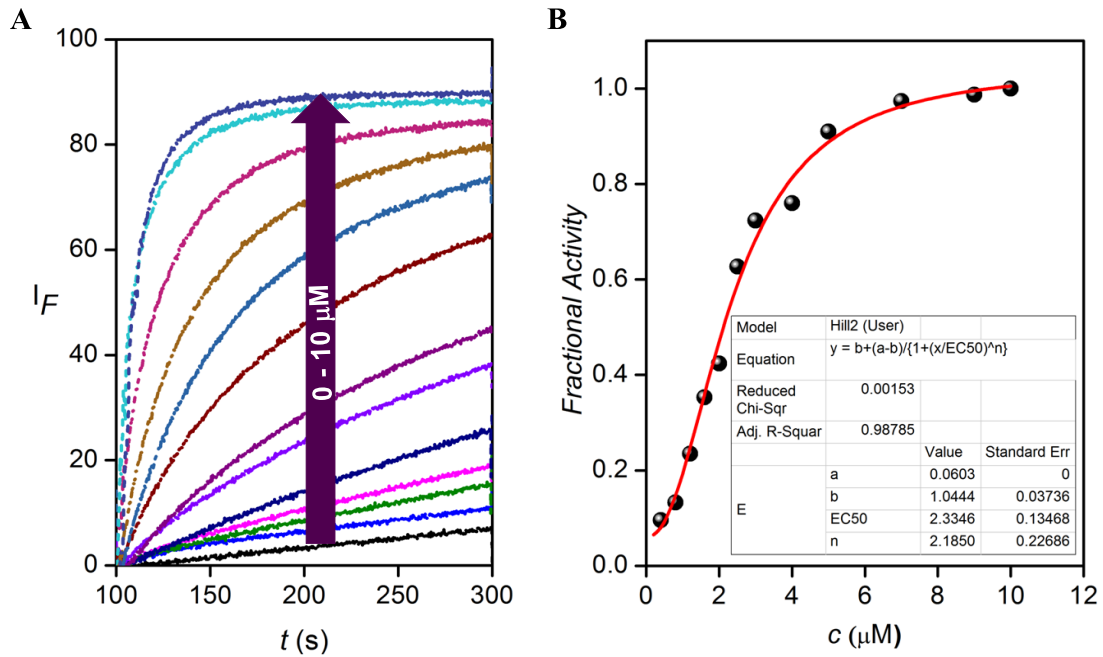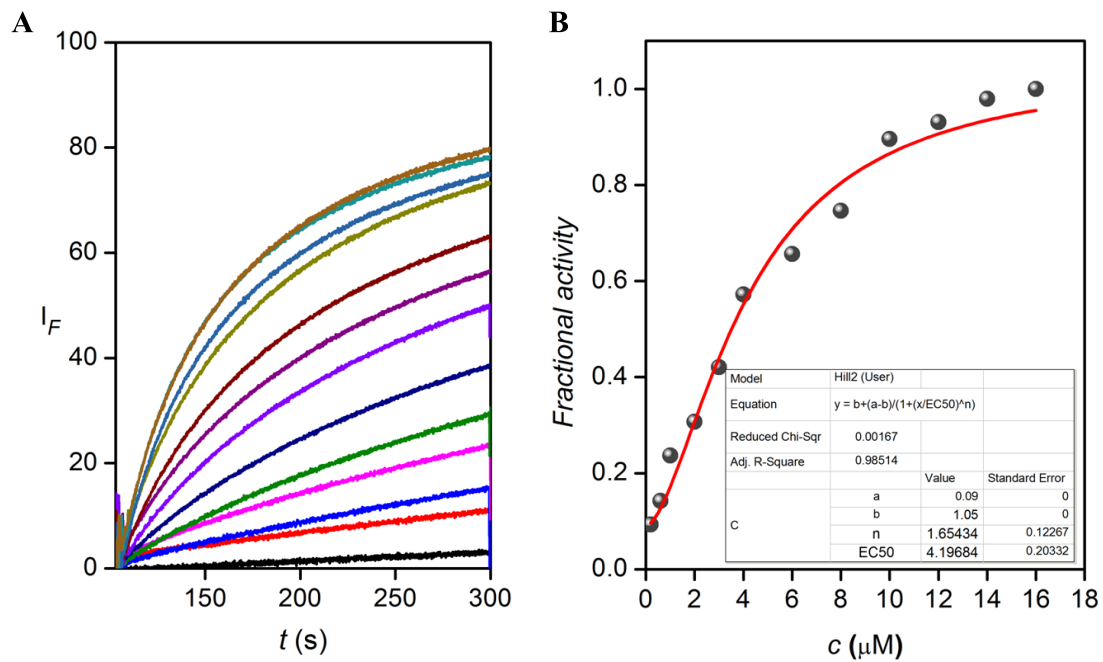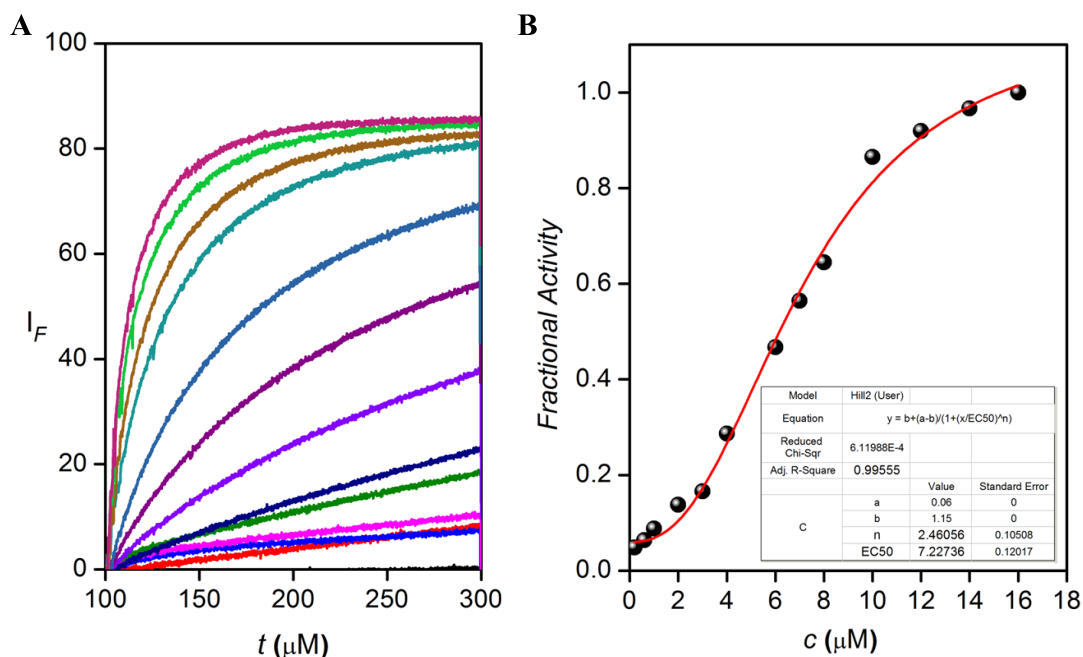ation to form a thin film. The formed thin film of lipid then dried under vacuum for >3 h. The resulting films were hydrated with 1 ml buffer A (12.5 mM ANTS, 45.0 mM DPX, 5 mM Tes, and 20 mM KCl, pH 7.0 for more than 60 minutes with occasional vortexing at 10 minute interval and then subjected to 7 freeze–thaw cycles and extrusions (15·time, Mini-Extruder with two stacked polycarbonate membranes, pore size 100 nm). Extravesicular dyes were removed by gel filtration (Sephadex G-50) eluting with buffer B (5 mM Tes, 100 mM KCl, pH 7.0). The collected LUV fraction was diluted to 6 ml with buffer B (5 mM Tes, 100 mM KCl, pH 7.0). The final stock solutions had the following characteristics: ~ 5 mM EYPC, Inside: 12.5 mM ANTS, 45.0 mM DPX, 5 mM Tes, 20 mM KCl, pH 7.0; outside: 5 mM Tes, 100 mM KCl, pH 7.0.

D. Vesicle leakage assay:

In a clean and dry fluorescence cuvette, 1950 μL of buffer (5 mM Tes, 100 mM KCl, pH 7.0) was added followed by the addition of 50 μL EYPC-LUV⊃ANTS/DPX vesicles suspension from above stack. The resulting solution was slowly stirred with the magnetic stirrer equipped with the fluorescence instrument. The time-dependent change in fluorescence intensity at λ_{em} =

520 nm was monitored at excitation wavelength λ_{ex} = 353 nm during the addition of transporter molecule **1d** as DMSO solution at t = 50 s, and finally 5% Trion X-100 (25 μL) at t = 300 s was added to lyse the vesicles so that the complete destruction of pH gradient is achieved (Fig. S41). The collected data was then normalized to the percentage change in fluorescence intensity as a course of time using the equation 1:
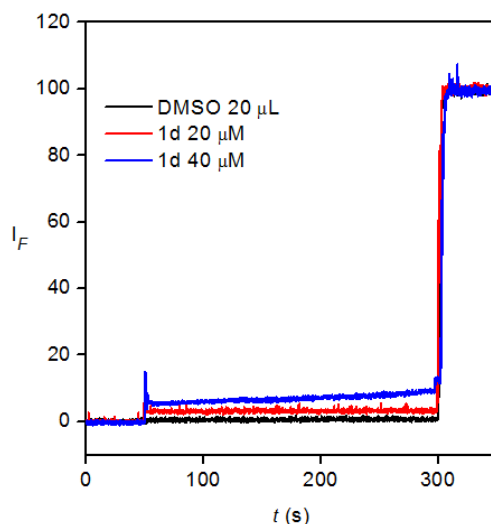

Fig. 40 Change in ANTS fluorescence (λ_{em} = 520 nm, λ_{ex} = 353 nm) upon addition of **1d** (20-40 μM) to EYPC LUVs⊃ANTS/DPX, fluorescence intensity calibrated to I_F = 100 after final lysis.

E. Ion Selectivity Studies Across EYPC-LUV⊃HPTS.

Preparation of EYPC-LUVs⊃HPTS: Vesicles were prepared according to the same procedure as stated above.

Anion selectivity assay:[S8] In a clean and dry fluorescence cuvette, 1975 μL of HEPES buffer (10 mM HEPES, 100 mM NaA, pH = 7.0; where, A^- = Cl^-, Br^-, I^-, NO_3^- , OAc^-, and ClO_4^-) was added followed by addition of 25 μL of EYPC-LUVs⊃HPTS in slowly stirring condition by a magnetic stirrer equipped with the fluorescence instrument (at t = 0 s). The HPTS fluorescence emission intensity, I_F was observed at λ_{em}= 510 nm (λ_{ex} = 450 nm) with time. 20 μL of 0.5 M NaOH was added to the cuvette at t = 20 s to create the pH gradient (ΔpH ~0.8) between the intra and extravesicular system. Transporter compounds were added at t = 100 s and of 10% Triton X-100 (25 μL) was added at t = 300 s to lyze vesicles for the complete destruction of pH gradient. The collected data was then normalized to the percentage change in fluorescence intensity as a course of time using the equation S1.

Cation selectivity:[S8] Similar to anion, the cation selectivity assay was performed by varying the extravesicular cations as metal chloride salts i.e. MCl, where, M$^+$ = Li$^+$, Na$^+$, K$^+$, Rb$^+$, Cs$^+$. No change in transport activity was observed for different cations.
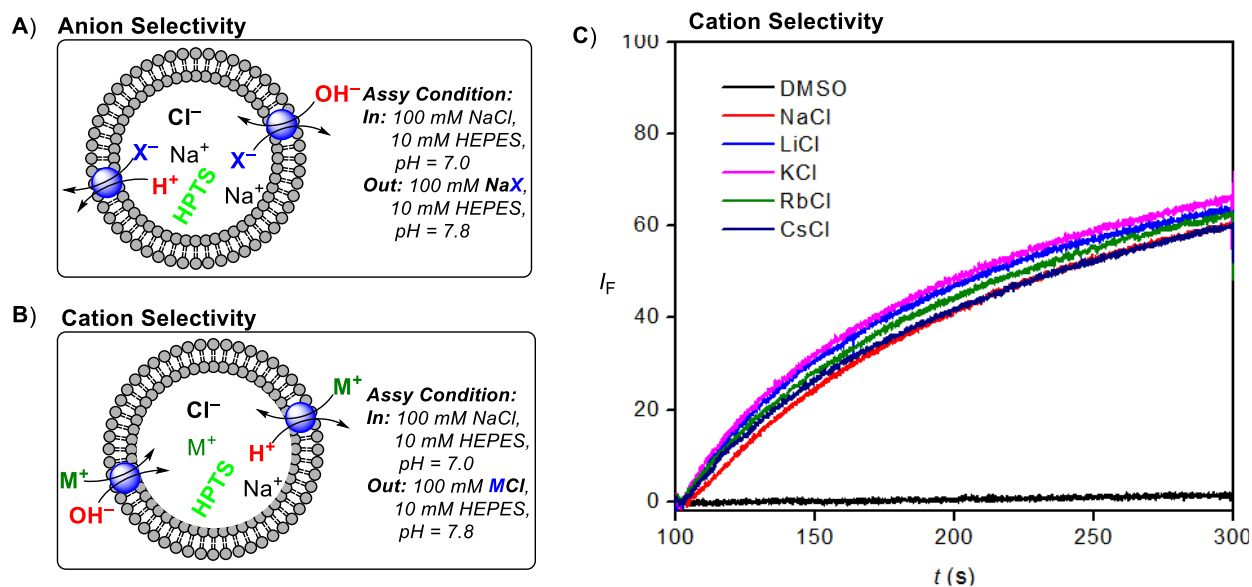

Fig. S41 Representative assay conditions, for anion selectivity (**A**), Cation selectivity (**B**), and cation selectivity of **1a** (2.5 μM) measured by varying the extravesicular cations (**C**).

Anion selectivity assay without pH gradient:[S8] The vesicles prepared using the same protocol as discussed in section SVIIA. In a clean and dry fluorescence cuvette, 1975 μL of HEPES buffer (10 mM HEPES, 100 mM NaA, pH = 7.0; where, A$^-$ = Cl$^-$, Br$^-$, I$^-$, NO$_3^-$, ClO$_4^-$, SO$_4^-$) was added followed by addition of 25 μL of EYPC-LUVs⊃HPTS in slowly stirring condition by a magnetic stirrer equipped with the fluorescence instrument (at t = 0 s). The HPTS fluorescence emission intensity, I_F was observed at λ_{em}= 510 nm (λ_{ex} = 450 nm) with time. Transporter compounds were added at t = 50 s and of 10% Triton X-100 (25 μL) was added at t = 300 s to lyze vesicles for the complete destruction of pH gradient. The collected data was then normalized to the percentage change in fluorescence intensity as a course of time using the equation S1.

The transporter molecule have an acidic proton (-SO$_2$NH-) having calculated pK_a of 7.4. Thus when the compound is added, there may be deprotonation of the sulfonamide proton causing the intravesicular pH drop followed by slow increase in fluorescence to equilibrium state by the active transporters **1d** (pK_a = 7.4) and **1f** (pK_a = 7.5) caused by H$^+$/Cl$^-$ symport. However the acidic receptor **1a** (pK_a = 5.6) did gain equilibrium state (Fig. 42).
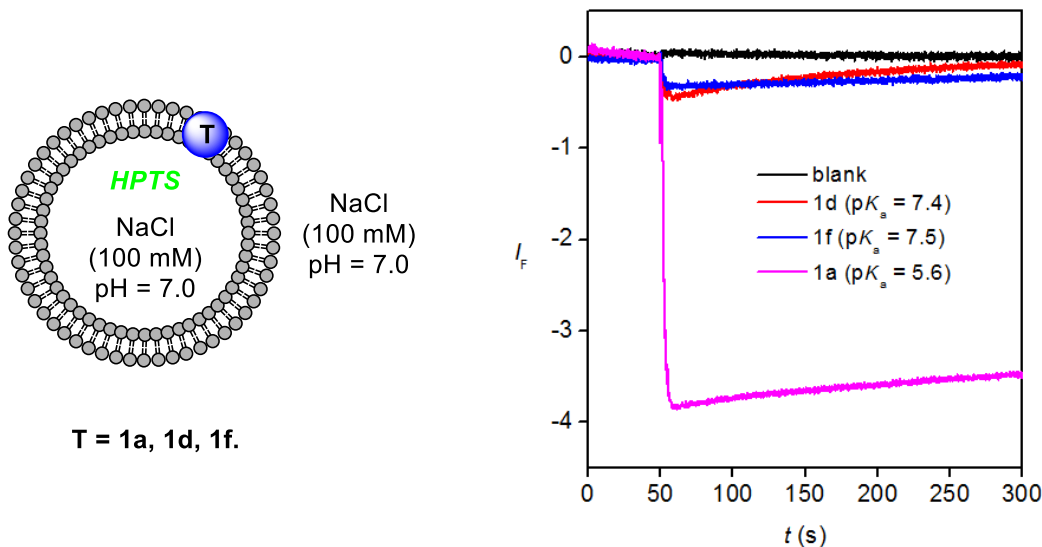
Fig. S42 The changes in the intravesicular pH across EYPC-LUVs⊃HPTS (inside: 10 mM HEPES, 100 mM NaCl, 1 mM HPTS, pH = 7.0) suspended in buffer (i.e extravesicular: 10 mM HEPES, 100 mM NaCl, 1 mM HPTS, pH = 7.0) opon addition of **1a**, **1d** and **1f**.

F. Preparation of EYPC-LUVs⊃lucigenin Vesicle:[S10] In a small clean and dry round bottom flask a transparent thin film of egg yolk phosphatidylcholine (EYPC) was prepared by drying a 1 mL of EYPC lipid (25 mg/ ml in CHCl$_3$) with continuous rotation and purging of nitrogen gas. The transparent film formed was kept in high vacuum for 4h to remove all the traces of CHCl$_3$. The transparent lipid film was rehydrated with 1 mL of buffer (Sodium phosphate 5mM, NaNO$_3$ 200 mM, 1 mM lucigenin, pH 7) solution and resulting suspension was vortexed at an interval of 10 minutes during period of 60 minutes and subjected to ≥10 freeze-thaw cycles (liq. N$_2$, 55 °C water bath), and >19 times (must be an odd number) extruded through a polycarbonate membrane (pore size 200 nm). Extravesicular dye was removed by size exclusion chromatography using Sephadex G-50 (Sigma Aldrich) eluting with aqueous NaNO$_3$ (200 mM) and diluted to 3 mL.

In a clean and dry fluorescence cuvette, 1975 µL of buffer (5 mM Na-phosphate, 200 mM NaNO$_3$, pH 7.0) was added, followed by the addition of 25 µL EYPC-LUV⊃Lucigenin. The resulting solution was slowly stirred with the magnetic stirrer equipped with the fluorescence instrument. The time-dependent change in fluorescence intensity at λem = 510 nm was monitored by excitation at wavelength λ$_{ex}$ = 455 nm during the addition of NaCl (33 mM to create Cl$^-$ gradient) at t = 20 s, (In valinomycin coupled assay, valinomycin added at 50 sec) transporter molecule in acetonitrile solution added at t = 100 Sec, and finally 10% Trion X-100 (25 µl,) at t = 300 s was added to lyse the vesicle resulting in complete destruction of chloride gradient. The collected data was then normalized to the percentage change in fluorescence intensity as a course of time using the equation 3.

$$I_F = (I_t - I_0)/(I_\infty - I_0) \times (-100) \qquad\qquad \text{Equation 3.}$$

Where, I_0 is the initial intensity, I_t is the intensity at time t, and I_∞ is the final intensity after addition of Triton X-100.

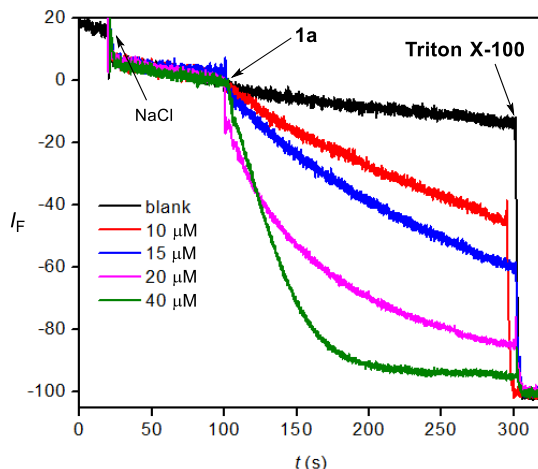**Fig. S43** Cl⁻ ion transport activity across EYPC-LUVs⊃lucigenin with increasing concentration of **1d** (0-40 µM)

G. FCCP and Valinomycin assay

FCCP Assay:[S9]
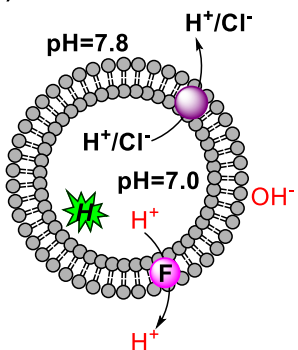
Fig. S44 Representative fluorescence-based FCCP coupled assay using EYPC-LUV (**A**) and representation of ion transport kinetics showing normalization window (**B**).

The Vesicles were prepared by following the same procedure as mentioned above. The data were recorded with and without FCCP. In a clean and dry fluorescence cuvette, 1975 µL of buffer (10

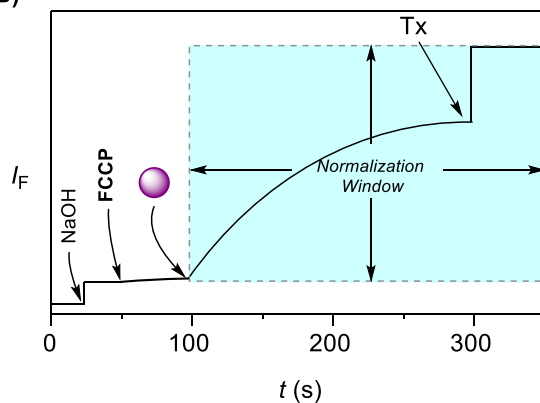mM HEPES, 100 mM NaCl, pH 7.0) was added, followed by the addition of 25 µL EYPC-LUV⊃HPTS dye. The resulting solution was slowly stirred with the magnetic stirrer equipped with the fluorescence instrument. The time-dependent change in fluorescence intensity at λ_{em} = 510 nm was monitored by excitation at wavelength λ_{ex} = 450 nm during the addition of base (20 µL, 0.5 M NaOH to create pH gradient) at t = 20 s, FCCP (0.8 µM) at 50 s, transporter molecule in DMSO solution at t = 100 s, and finally 10% Triton X-100 (25 µL) at t = 300 s was added to lyse the vesicle resulting in complete destruction of pH gradient. The collected data was then normalized to the percentage change in fluorescence intensity as a course of time using the equation S1. It was observed that the presence of FCCP did not enhance transport rate, demonstrating that ion transport mechanism involves the symport process, probably H^+/Cl^- symport which delegates the charge balance.
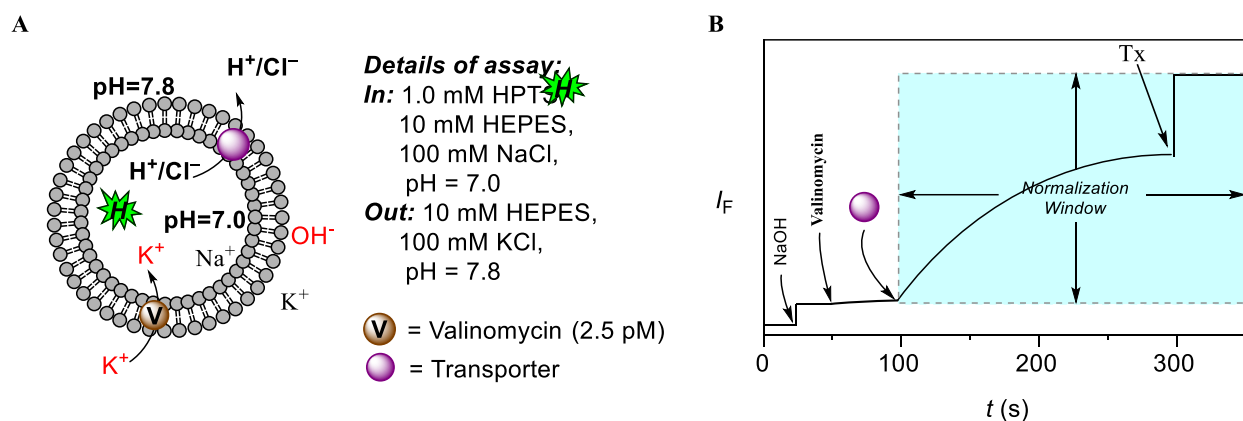
Valinomycin Assay:[S9]

Fig. S45 Representative fluorescence-based Valinomycin coupled assay using EYPC-LUV (**A**), and representation of ion transport kinetics showing normalization window (**B**).

The vesicles were prepared by following the same procedure as mentioned above. The data were recorded with and without the addition of valinomycin. In a clean and dry fluorescence cuvette, 1975 µL of buffer (10 mM HEPES, 100 mM KCl, pH 7.0) was added, followed by the addition of 25 µL EYPC-LUV⊃HPTS dye. The resulting solution was slowly stirred with the magnetic stirrer equipped with the fluorescence instrument. The time-dependent change in fluorescence intensity at λ_{em} = 510 nm was monitored by excitation at wavelength λ_{ex} = 450 nm during the addition of base (20 µL, 0.5 M NaOH to create pH gradient) at t = 20 s, valinomycin (2.5 µM) at 50 s, transporter molecule in DMSO solution at t = 100 s and finally 10% Triton X-100 (25 µL) was added at t = 300 s to lyse the vesicle resulting in complete destruction of pH gradient. The collected data was then normalized to the percentage change in fluorescence intensity as a course of time using the equation S1.

H. The Ion Transport across Transport across EYPC-LUVs⊃HPTS, (10 mM HEPES, 100 mM NaNO₃, pH = 7.0):[S11,S12] The vesicles were prepared by entrapping the HPTS dye and NO$_3^-$ ions inside the vesicles (EYPC-LUVs⊃HPTS, 10 mM HEPES, 100 mM NaNO3, pH = 7.0). The vesicles were suspended in the either buffer **A** (10 mM HEPES, 100 mM NaNO3, pH = 7.0) or buffer **B** (10 mM HEPES, 100 mM NaCl, pH = 7.0). In the former case [i.e. EYPC-LUVs⊃HPTS (10 mM HEPES, 100 mM NaNO₃, pH = 7.0) suspended in buffer A], the addition of compound **1d** resulted in a rapid drop in the fluorescence intensity indicative of H$^+$/NO$_3^-$ influx, and then slow increase of fluorescence to the fully equilibrated state. However, in later case [i.e. EYPC-LUVs⊃HPTS (10 mM HEPES, 100 mM NaCl, pH = 7.0) suspended in buffer **B**], the addition of compound **1d** resulted in a rapid increase in the fluorescence intensity indicative of H$^+$/NO$_3^-$ efflux, instead of H$^+$/Cl$^-$ influx. This data indicate that, even in the symmetrical pH solution, the symport mechanism is operative and not a NO$_3^-$/Cl$^-$ exchange. The data also suggest that in the symmetrical pH solution **1d** transports NO$_3^-$ preferentially over the Cl$^-$. However, the symport process is the main transport mechanism for **1d**.
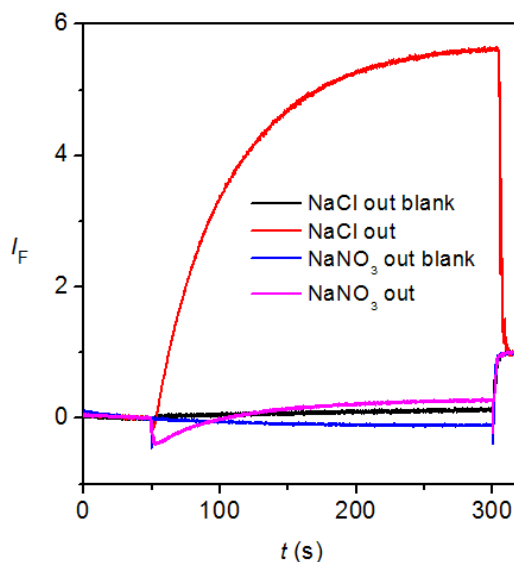

Fig. S46 The changes in the intravesicular pH across EYPC-LUVs⊃HPTS (inside: 10 mM HEPES, 100 mM NaNO3, 1 mM HPTS, pH = 7.0). The Vesicle was suspended in either NaCl or NaNO₃ containing buffer of pH = 7.0 and changes in intravesicular pH were monitored after addition of compound **1d** (A).

SVIII. Mass Spectrometric Evidence of Anion Binding

Experimental Details: The samples were prepared in acetonitrile by varying the ratio of **1d** and Cl$^-$. The samples were electrosprayed as 20 µM solutions of **1d** and TBACl (TMACl) in acetonitrile at flow rates of 0.4 mL/min. A constant spray and highest intensities were achieved

with a capillary voltage of 3000 V at a source temperature of 80 °C. The parameters for sample cone (40 V) and extractor cone voltage (5 V) were optimized for maximum intensities of the desired complexes. Fig. S47 represents the ESI-MS data recorded from acetonitrile solution of **1d** with TMACl prepared in 1:1 molar ratio. From the spectrum, signals corresponding to [M+2TBA+Cl]$^+$ was detected.
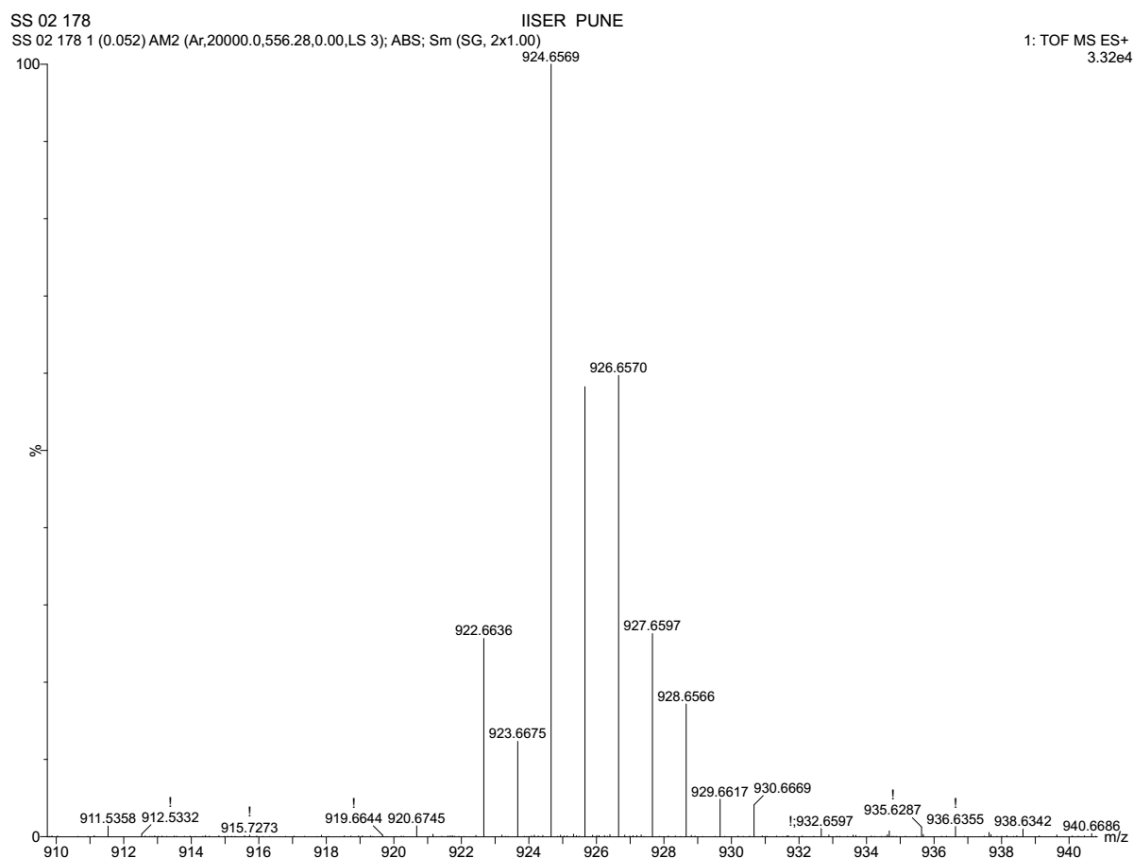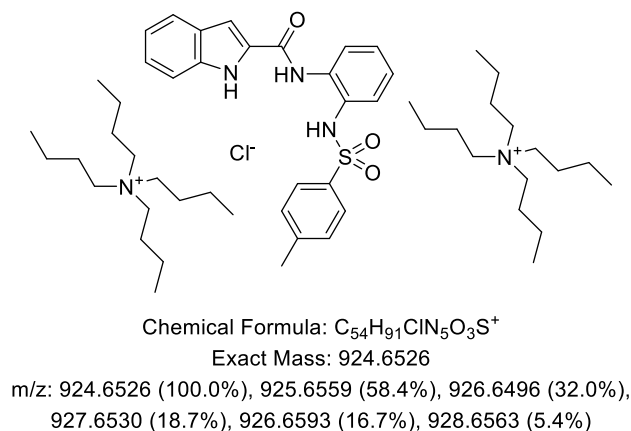

Chemical Formula: $C_{54}H_{91}ClN_5O_3S^+$
Exact Mass: 924.6526
m/z: 924.6526 (100.0%), 925.6559 (58.4%), 926.6496 (32.0%),
927.6530 (18.7%), 926.6593 (16.7%), 928.6563 (5.4%)

Fig. S47 HRMS spectrum of compound **1d** + TBACl.

SIX. References.

S1. L. Xi, J.-Q. Zhang, Z.-C. Liu, J.-H. Zhang, J.-F. Yan, Y. Jin and J. Lin, *Org. Biomol. Chem.*, 2013, **11**, 4367-4378.

S2. R. Taylor and O. Kennard, *J. Am. Chem. Soc.*, 1982, **104**, 5063-5070.

S3. G. R. Desiraju, *Mol. Cryst. Liq. Cryst. Sci. Technol., Sect. A*, 1992, **211**, 63-74.

S4. M. J. Turner, J. J. McKinnon, S. K. Wolff, D. J. Grimwood, P. R. Spackman, D. Jayatilaka and M. A. Spackman, *CrystalExplorer17* (2017).

S5. J. J. McKinnon, A. S. Mitchell and M. A. Spackman, *Chem. – Eur. J.*, 1998, **4**, 2136-2141.

S6. J. J. McKinnon, D. Jayatilaka and M. A. Spackman, *Chem. Commun.*, 2007, 3814-3816.

S7. S. Shit, C. Marschner and S. Mitra, *Acta Chim. Slov.*, 2016, **63**, 129-137.

S6. M. J. Hynes, *J. Chem. Soc., Dalton Trans.*, 1993, 311-312.

S7. K. Kano and J. H. Fendler, *Biochim. Biophys. Acta, Biomembr.*, 1978, **509**, 289-299.

S8. N. Sakai and S. Matile, *J. Phys. Org. Chem.*, 2006, **19**, 452-460.

S9. S. V. Shinde and P. Talukdar, *Angew. Chem., Int. Ed.*, 2017, **56**, 4238-4242.

S10. B. A. McNally, A. V. Koulov, B. D. Smith, J.-B. Joos and A. P. Davis, *Chem. Commun.*, 2005, 1087-1089.

S11. P. I. Hernandez, D. Moreno, A. A. Javier, T. Torroba, R. P.-Tomas, and R. Quesada, *Chem. Commun.,* 2012, **48**, 1556-1558.

S12. J. L. Seganish and J. T. Davis, *Chem. Commun.*, 2005, **46**, 5781-5783.